Mitochondrial Nicotinamide Nucleotide Transhydrogenase : Role in Energy Metabolism, Redox Homeostasis, and Cancer

Antioxidants and redox signaling

Gan, Zhuohui; van der Stelt, Inge; Li, Weiwei; Hu, Liangyu; Song, Jingyi et al

https://doi.org/10.1089/ars.2024.0694

ANTIOXIDANTS & REDOX SIGNALING
Volume 41, Numbers 13–15, 2024

DOI: 10.1089/ars.2024.0694

FORUM REVIEW ARTICLE

Mitochondrial Nicotinamide Nucleotide Transhydrogenase: Role in Energy Metabolism, Redox Homeostasis, and Cancer

Zhuohui Gan,[1,*] Inge van der Stelt,[1,*] Weiwei Li,[1,*] Liangyu Hu,[1] Jingyi Song,[1] Sander Grefte,[1] Els van de Westerlo,[2,3] Deli Zhang,[1] Evert M. van Schothorst,[1] Hedi L. Claahsen-van der Grinten,[4] Katja J. Teerds,[1] Merel J.W. Adjobo-Hermans,[2,3] Jaap Keijer,[1,†] and Werner J.H. Koopman[1,3,4,†]

Abstract

Significance: Dimeric nicotinamide nucleotide transhydrogenase (NNT) is embedded in the mitochondrial inner membrane and couples the conversion of $NADP^+$/NADH into NADPH/NAD^+ to mitochondrial matrix proton influx. NNT was implied in various cancers, but its physiological role and regulation still remain incompletely understood.

Recent Advances: NNT function was analyzed by studying: (1) *NNT* gene mutations in human (adrenal) glucocorticoid deficiency 4 (GCCD4), (2) *Nnt* gene mutation in C57BL/6J mice, and (3) the effect of NNT knockdown/overexpression in (cancer) cells. In these three models, altered NNT function induced both common and differential aberrations.

Critical Issues: Information on NNT protein expression in GCCD4 patients is still scarce. Moreover, NNT expression levels are tissue-specific in humans and mice and the functional consequences of NNT deficiency strongly depend on experimental conditions. In addition, data from intact cells and isolated mitochondria are often unsuited for direct comparison. This prevents a proper understanding of NNT-linked (patho)physiology in GCCD4 patients, C57BL/6J mice, and cancer (cell) models, which complicates translational comparison.

Future Directions: Development of mice with conditional *NNT* deletion, cell-reprogramming-based adrenal (organoid) models harboring specific *NNT* mutations, and/or NNT-specific chemical inhibitors/activators would be useful. Moreover, live-cell analysis of NNT substrate levels and mitochondrial/cellular functioning with fluorescent reporter molecules might provide novel insights into the conditions under which NNT is active and how this activity links to other metabolic and signaling pathways. This would also allow a better dissection of local signaling and/or compartment-specific (*i.e.,* mitochondrial matrix, cytosol, nucleus) effects of NNT (dys)function in a cellular context. *Antioxid. Redox Signal.* 41, 927–956.

Keywords: NNT, mitochondria, bioenergetics, redox homeostasis, experimental models, cancer

Introduction

Mitochondria, classically recognized as adenosine triphosphate (ATP) producers, consist of a highly folded mitochondrial inner membrane (MIM) and outer membrane (MOM) that envelop an aqueous matrix compartment (Bulthuis et al., 2023). These organelles display interlinked dynamic changes in their morphology and function (“morphofunction”) and also play crucial roles in cell physiological processes not directly related to ATP generation (Weinberg et al., 2015; Bulthuis et al., 2019). The latter includes reactive oxygen species (ROS) production, calcium (Ca^{2+}) homeostasis, apoptosis

[1]Human and Animal Physiology, Wageningen University, Wageningen, The Netherlands.
[2]Department of Medical BioSciences, Radboudumc, Nijmegen, The Netherlands.
[3]Radboud Center for Mitochondrial Medicine, Radboudumc, Nijmegen, The Netherlands.
[4]Department of Pediatrics, Amalia Children’s Hospital, Radboudumc, Nijmegen, The Netherlands.
*Joint first authors.
†Joint senior authors.

induction, and inflammatory responses. Therefore, it is not surprising that mutations in mitochondrial protein-encoding genes, as well as other external factors inducing mitochondrial dysfunction, are linked to both (rare) mitochondrial disorders and more common human pathologies, including diabetes, neurodegeneration, and Parkinson's disease (Koopman et al., 2012; Janssen Daalen et al., 2023). With the aim to complement other works (Vercesi et al., 2018; Nesci et al., 2020; Francisco et al., 2022; Regan et al., 2022; Grayson and Mailloux, 2023), we here review the current knowledge regarding the nicotinamide nucleotide transhydrogenase (NNT). This MIM-embedded pyridine nucleotide transhydrogenase connects mitochondrial energy metabolism and redox homeostasis (*e.g.,* Danielson and Ernster, 1963; Kampjut and Sazanov, 2019). Detailed descriptions of the NNT atomic structure and molecular mechanism are provided elsewhere (Chen and Guillory, 1984; Persson et al., 1987; White et al., 2000; Cotton et al., 2001; Jackson, 2012; Leung et al., 2015; Metherell et al., 2016; Kampjut and Sazanov, 2019). Here, we first present a short primer regarding mitochondrial energy and ROS homeostasis (see sections "Mitochondrial bioenergetics" and "Role of mitochondria in ROS homeostasis"), followed by an overview of NNT gene/protein structure, function, and regulation (see section "The mitochondrial nicotinamide nucleotide transhydrogenase"). Next, we review NNT mutations and their consequences in human patients (see section "*NNT* gene mutations and disease in humans"), as well as the impact of *Nnt* gene mutation in C57BL/6J mice (see section "Impact of *Nnt* gene mutations in C57BL/6J mice"). Then we discuss the results of NNT functional analyses in cell and other models (see section "Analysis of NNT function in other models"). In the context of the above, we present the current state-of-the-art regarding the role of NNT in various forms of cancer (see section "Role of NNT in cancer cells").

Mitochondrial bioenergetics

Glucose generally represents the initial substrate for mitochondrial ATP generation (Fig. 1A). Following entry into the cell *via* glucose transporters, glucose feeds into the glycolysis pathway to generate ATP and reduced nicotinamide adenine dinucleotide (NADH) and pyruvate. Other monosaccharides such as galactose and fructose also can be glycolytically converted into pyruvate. In case of galactose, this conversion requires the Leloir pathway (Holden et al., 2003) and occurs at a lower rate relative to glucose (Iannetti et al., 2018). Importantly, glycolysis interfaces with other metabolic pathways, including amino acid metabolism and redox homeostasis (*via* the pentose phosphate pathway; PPP). When glycolysis is highly active, for instance, during mitochondrial dysfunction and/or high cellular proliferation rates, excess amounts of pyruvate can be converted into lactate, which is then transported out of the cell, potentially acidifying the extracellular environment (Fig. 1A). Normally, the majority of pyruvate enters mitochondria (Fig. 1B), where it is converted into acetyl coenzyme A (AcCoA) to fuel ATP production by the integrated action of the tricarboxylic acid (TCA) cycle (Fig. 1C) and the oxidative phosphorylation (OXPHOS) system (Fig. 1D). The conversion of pyruvate into AcCoA by pyruvate dehydrogenase (PDH) is irreversible and therefore carbohydrates can be converted into fats but not *vice versa* (Frayn and Evans, 2019). Depending on the cell type and/or (patho)physiological condition, ATP also can be (co)produced from alternative substrates such as glutamine and fatty acids (FAs) entering the TCA cycle (Fig. 1C; Goodpaster and Sparks, 2017). Mitochondrial ATP production is sustained by the action of the electron transport chain (ETC), which is embedded in the MIM (Fig. 1D). The ETC consists of four complexes (CI–CIV), which abstract electrons from NADH (generating NAD^+ at CI) and succinate (generating reduced flavin adenine dinucleotide at CII). These electrons are subsequently transported to CIII (mediated by coenzyme Q10; CoQ10) and to CIV (mediated by cytochrome-*c*; CYTC). At CIV, electrons are donated to oxygen (O_2)-inducing formation of water (H_2O). Energy generated during electron transport is utilized to expel protons (H^+) from the mitochondrial matrix across the MIM (at CI, CIII, and CIV). As a consequence, the matrix becomes more alkaline, leading to a trans-MIM pH difference (ΔpH), and an inside-negative trans-MIM membrane potential ($\Delta\psi$). Together, $\Delta\psi$ and ΔpH sustain a matrix-directed proton-motive force (PMF). The latter is utilized by the fifth complex (CV or F_oF_1-ATPase), which mediates the controlled backflow of H^+ into the mitochondrial matrix, to generate ATP from adenosine diphosphate (ADP) and inorganic phosphate (P_i; Mitchell and Moyle, 1967). Together, the ETC and CV constitute the mitochondrial OXPHOS system (Fig. 1D). Electrons can also enter the ETC *via* alternative pathways, often in a tissue-specific manner. Examples of such pathways are the electron donation to CoQ10 by glycerol-3-phosphate (G3P) dehydrogenase (GPDH), dihydroorotate dehydrogenase (DHODH), and the electron-transferring flavoprotein (ETF)-ubiquinone oxidoreductase (ETFQO; a.k.a ETFDH; Koopman et al., 2010). Cellular ATP generation is highly flexible and can rapidly switch from mitochondrial OXPHOS- to glycolysis-mediated ATP production when the former pathway is impaired (Liemburg-Apers et al., 2015; Liemburg-Apers et al., 2016; Bulthuis et al., 2022). In addition to ATP generation, ETC action also sustains virtually all other mitochondrial functions, including preprotein import (Fig. 1E) and metabolite/ion exchange (Fig. 1B, F). These functions are discussed in detail elsewhere (*e.g.,* Koopman et al., 2010; Bulthuis et al., 2019; Szabo and Szewczyk, 2023).

Role of mitochondria in ROS homeostasis

Importantly, mitochondria can produce ROS as by-products of ETC action (Fig. 1G), in particular during pathological conditions (Chenna et al., 2022). Using chemical inhibitors, 12 mitochondrial production sites of the ROS hydrogen peroxide (H_2O_2) were highlighted (Grayson and Mailloux, 2023): α-ketoglutarate (oxoglutarate) dehydrogenase (α-KGDH; a.k.a. 2-oxoglutarate dehydrogenase complex component E1 [OGHD]), branched chain ketoacid dehydrogenase, CI (2 sites), CII, CIII, DHODH, ETFQO, oxoadipate dehydrogenase, PDH, proline dehydrogenase, and *sn*-GPDH. A detailed overview of the applied inhibitors and experimental conditions is provided in the original study (Grayson and Mailloux, 2023). H_2O_2 and other ROS can act as messenger molecules in physiological cell control and/or induction of antioxidant signaling (Willems et al., 2015; Sieprath et al., 2016; Teixeira et al., 2021). However, when ROS levels become too high, they induce oxidative stress through damaging biomolecules and/or altering redox homeostasis (Halliwell

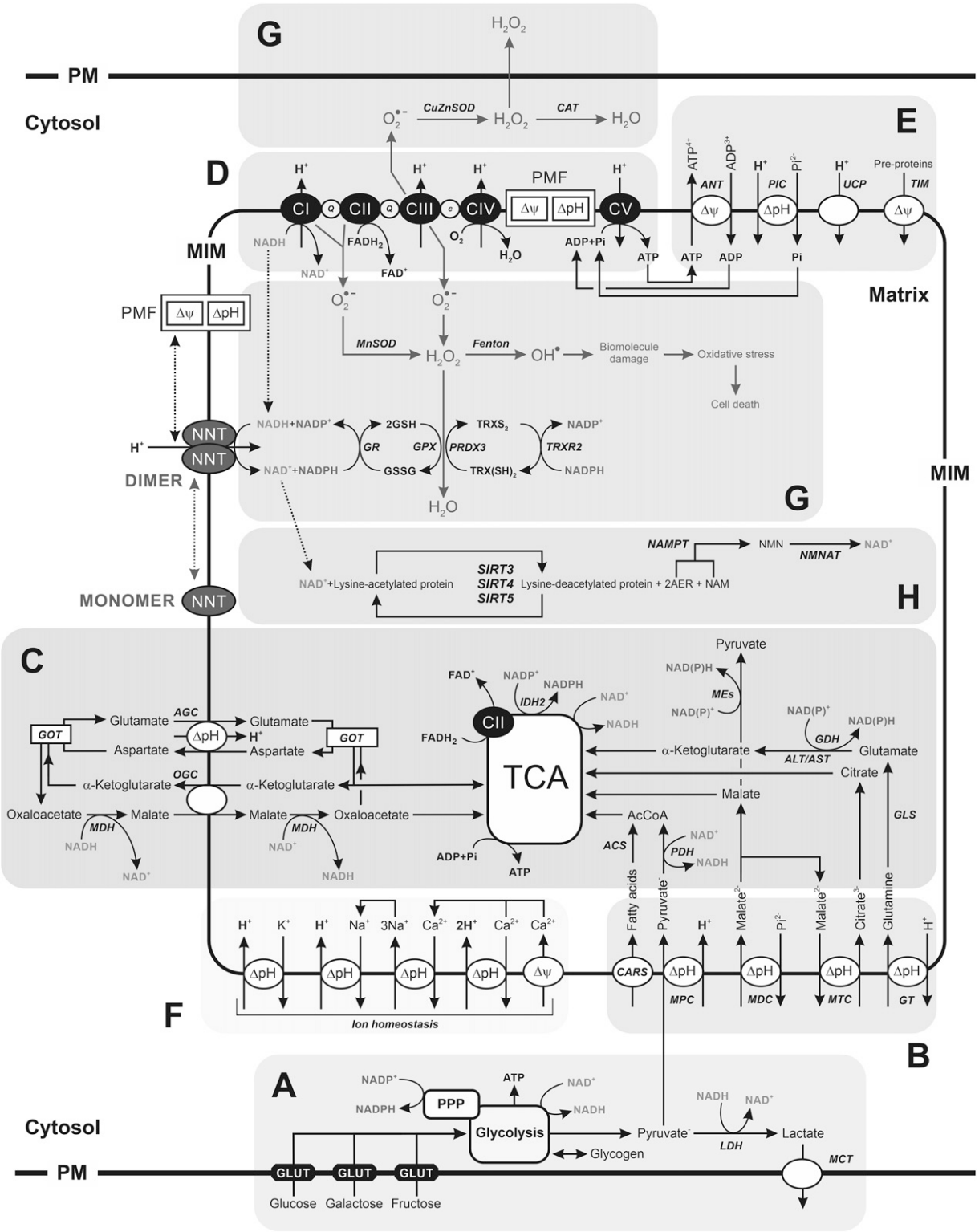

FIG. 1. Integration of mitochondrial NNT function in cellular energy metabolism and redox homeostasis. Different aspects of integrated cellular energy and ROS/redox metabolism are highlighted (see main text for details). The MOM and IMS are omitted for visualization purposes. Specific parts of this system are indicated: **(A)** Cellular metabolite entry and glycolysis, **(B)** mitochondrial metabolite exchange, **(C)** TCA cycle-linked systems, **(D)** OXPHOS system, **(E)** OXPHOS-linked ATP/ADP/P_i exchange, uncoupling proteins, and preprotein import, **(F)** mitochondrial ion exchange, **(G)** ROS/redox metabolism, **(H)** SIRT-mediated protein deacetylation. This figure was compiled from (Huang et al., 2006; Koopman et al., 2010; Monné et al., 2013; Krengel and Törnroth-Horsefield, 2015; Ronchi et al., 2016; Scalise et al., 2016; Sieprath et al., 2016; van de Ven et al., 2017; Console et al., 2020; Nesci et al., 2020; Xiao and Loscalzo, 2020; Yoo et al., 2020; Chenna et al., 2022; Qu et al., 2021). ATP/ADP/Pi, adenosine triphosphate/adenosine diphosphate/inorganic phosphate; IMS, intermembrane space; MOM, mitochondrial outer membrane; NNT, nicotinamide nucleotide transhydrogenase; OXPHOS, oxidative phosphorylation; ROS, reactive oxygen species; SIRT, sirtuin; TCA, tricarboxylic acid.

and Gutteridge, 2015). Under nonpathological conditions, mitochondrial oxidative stress is effectively antagonized by various interlocking antioxidant systems (Fig. 1G). These include manganese superoxide dismutase (MnSOD a.k.a. SOD2), glutathione reductase (GR), glutathione peroxidases (GPXs), peroxiredoxins (PRDXs), and thioredoxin reductases (TRXRs). Importantly, the reduced form of nicotinamide adenine dinucleotide phosphate (NADPH) functionally sustains several of the above-mentioned systems (Fig. 1G) and is (co)generated by NNT.

The Mitochondrial NNT

The NNT/Nnt gene

In humans (*Homo sapiens*) and mice (*Mus musculus*), the genetic information for the NNT protein is localized on the *NNT* gene (chromosome 5p12) and *Nnt* gene (chromosome 13D2), respectively. Both genes encode 22 exons, which contain a mitochondrial targeting sequence (MTS) and three NNT functional domains (Fig. 2). Domain I (dI) mediates the binding of NADH and NAD^+ in the mitochondrial matrix, domain II (dII) is the trans-MIM domain, and domain III (dIII) mediates the matrix binding of NADPH and $NADP^+$. In human and mouse, *NNT/Nnt* expression (mRNA levels) greatly differs between tissues (Fig. 3A, B). Integrating this information with data on CYTC levels in mouse tissues (Pagliarini et al., 2008) revealed a linear correlation with *Nnt* mRNA expression, in particular for the spleen, lung, placenta, liver, kidney, and heart (Fig. 3C). This suggests that *Nnt* expression levels scale with mitochondrial abundance/mass in these tissues.

The NNT protein

In humans (Q13423; UniProt; www.uniprot.org), mice (Q61941), and sheep (*Ovis aries*; W5PFI3), transcription of the *NNT*/*Nnt* gene yields a full-length NNT preprotein of 1086 amino acids (Fig. 4) The MTS (amino acids 1 to 43) of this preprotein is cleaved off after mitochondrial import, yielding a mature protein with a length of 1043 amino acids and a predicted molecular weight (MW) of ~109-kDa. Phospholipids stimulate the function of NNT (Rydström et al., 1976), which is catalytically active as a homodimer (Ormö et al., 1992; Kampjut and Sazanov, 2019). Although its exact dimerization mechanism is unknown, evidence in the bacterium *Rhodospirillum rubrum* suggests that tyrosine 146 in the NADH-binding (dI) part of NNT (*i.e.,* Y189 in the preprotein; Fig. 4) is important for dimer formation (Obiozo et al., 2007). Compatible with its catalytic function (see section "NNT function and redox homeostasis"), the binding sites for $NADH/NAD^+$, $NADPH/NADP^+$, and H^+ are highly conserved within the NNT dimer (Fig. 5). The NNT protein was readily detectable by Western blotting and widely expressed in C3H/HeJ mouse tissues (Ripoll et al., 2012). In this animal model, NNT protein levels increased in the following order: brain < kidney < lung < heart = skeletal muscle < liver < pancreas < bone marrow < spleen. This order does not fully correlate with *NNT* gene expression data (Fig. 3), compatible with the lack of correlation between *NNT* mRNA levels and NNT protein levels/activity in NNT-mutated patient cells (Francisco et al., 2024). Western blot tissue analysis of mice heterozygous for the wild-type (WT) *Nnt* allele (B6J-$Nnt^{W/T}$ mice) demonstrated that NNT protein levels were below or very close to the detection limit in skeletal muscle, lung, spleen, cortex, cerebellum, and brain stem (Kim et al., 2010). The latter study also reported that NNT protein levels increased in the following order: lung = skeletal muscle < liver < kidney $\ll$ heart, suggesting that the relative NNT protein level in tissues might (co)depend on the used mouse strain, physiological state, and/or experimental condition.

Post-translational modification of NNT

Analysis of the human and mouse protein sequence (Fig. 4 and Table 2) predicted various lysine post-translational modifications (PTMs). These consisted of two N6-acetyl-lysine positions (K70, K397) and five N6-succinyl-lysine positions (K117, K224, K294, K331, K1079). Similarly, experimental data from the Protein Lysine Modification Database (PLMD 3.0; http://plmd.biocuckoo.org/; Xu et al., 2017) also highlighted NNT lysine modifications (Table 2). The latter primarily consisted of acetylation and succinylation, but also included malonylation and ubiquitination. In the mature protein (*i.e.,* after MTS cleavage), all lysine modification sites were located within the matrix-protruding domains of NNT, rendering them accessible for potential PTM from within the mitochondrial matrix (Fig. 4). Acetylation, succinylation, and malonylation represent different types of acyl modifications that, in mitochondria, appear to be primarily driven by nonenzymatic mechanisms. This means that any unmodified lysine residue can react with acyl-CoA (variants) in the mitochondrial matrix in a concentration-dependent manner (Carrico et al., 2018). In the latter compartment, the reversal of these modifications (deacylation) is mediated by deacylases (sirtuins), in particular *via* SIRT3, SIRT4, and SIRT5. Interestingly, sirtuins are NAD^+-dependent enzymes (Fig. 1H; Guarente, 2011; van de Ven et al., 2017; Lin et al., 2018). This suggests the possibility that NNT and SIRTs constitute a homeostatic regulatory circuit, in which NNT regulates (local) NAD^+ levels and hence SIRT activity, whereas SIRTs regulate NNT-acetylation levels and thereby NNT activity. Supporting this idea, acetylome peptide microarray analysis demonstrated that SIRT4 displayed NAD^+-dependent deacetylation activity for NNT at K397 (Rauh et al., 2013). In addition to this autoregulatory mechanism, NNT-mediated modulation of (local) NAD^+ levels could affect various mitochondrial stress responses (https://haigis.hms.harvard.edu/mitochondrial-sirtuin-network; Yang et al., 2016). These involve the following (van de Ven et al., 2017): SIRT3 (impacting on ROS homeostasis, TCA cycle, OXPHOS, FA metabolism, amino acid metabolism, and ketone body metabolism), SIRT4 (urea cycle, mitochondrial unfolded protein response, mtDNA function, mitochondrial translation, and mitochondrial transporters), and SIRT5 (ROS homeostasis, TCA cycle, FA metabolism, and urea cycle). Analysis of submitochondrial particles suggested that NNT can also be oxidatively modified, and that endogenous ubiquinol might play a protective role in this process (Forsmark-Andrée et al., 1996). Moreover, it was reported that the NNT protein isolated from human heart mitochondria displayed 2,4-dinitrophenylhydrazine-related carbonylation, both during normal and pathophysiological conditions (Sheeran et al., 2010). Recently, ubiquitin-specific peptidase 47, a deubiquitinase,

FIG. 2. Human *NNT* gene structure and pathogenic mutations. *NNT* gene structure highlighting its 22 exons, N/C termini in the derived protein, mitochondrial targeting sequence (MTS), the three functional domains (dI, dII, dIII), and the missing exons in C57BL/6J mice. Pathogenic gene mutations are highlighted by vertical lines (Table 1). See main text for details.

was proposed as an NNT regulator (Li et al., 2023). Cancer-related PTMs of NNT are discussed below (see section "Role of NNT in cancer cells").

NNT function and redox homeostasis

Biochemically, NNT (EC 7.1.1.1) couples the conversion of (NADH + $NADP^+$) into (NAD^+ + NADPH) within the mitochondrial matrix to H^+ influx from the mitochondrial intermembrane space (IMS) into this matrix (Rydstrom, 2006; Fig. 1G):

$$H^+_{IMS} + NADH_{matrix} + NADP^+_{matrix} \rightleftarrows H^+_{matrix} + NAD^+_{matrix} + NADPH_{matrix} \quad \text{(Eq. I)}$$

NNT transfers electrons from NADH (yielding NAD^+) to $NADP^+$ (yielding NADPH) using the PMF as a driving force (Murphy, 2015; Vercesi et al., 2018). Since the PMF in

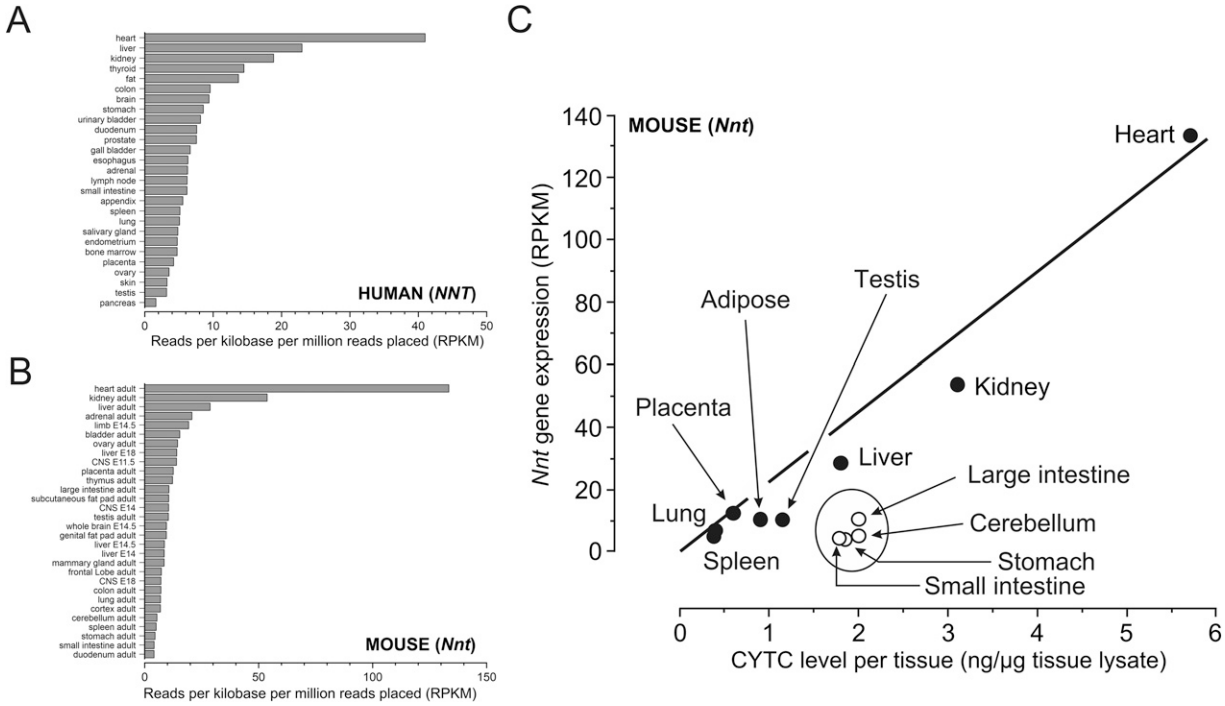

FIG. 3. NNT and Nnt gene expression in various tissues (A) *NNT* gene expression data (RNA-seq) in various human tissue samples from 95 individuals (www.ncbi.nlm.nih.gov/gene/23530). (B) Similar to panel A, but now for *Nnt* gene expression in various mouse tissues (www.ncbi.nlm.nih.gov/gene/18115). **(C)** Comparison of mouse tissue mitochondrial content (x-axis), expressed as cytochrome-c (CYTC) level in ng/µg tissue lysate (Pagliarini et al., 2008), and *Nnt* expression (y-axis; data taken from panel B). The thick line was manually drawn. Tissues in which *Nnt* expression was apparently not proportional to mitochondrial content are highlighted (oval).

Table 1. Pathogenic *Nicotinamide Nucleotide Transhydrogenase* Gene Mutations

ClinVar accession	*Mutation*		*Reference*
	cDNA	*Protein*	
265844	c.211C>T	p.Arg(R)71Ter (intron variant, nonsense)	Novoselova et al., 2015; Roucher-Boulez et al., 2016
265843	c.385C>T	p.Arg(R)129Ter (5′ UTR variant, nonsense)	Roucher-Boulez et al., 2016
265842	c.598G>A	p.Gly(G)200Ser(S)	Weinberg-Shukron et al., 2015
35539	c.600-601delG	Mutation at splice junction of intron 4 and exon5: (p.Tyr(Y)201Phefs*2	Meimaridou et al., 2012
265839	c.644T>C	p.Phe(F)215Ser(S) (missense)	Yamaguchi et al., 2013; Fujisawa et al., 2015
1705295	c.1089del	p.Leu(L)362Tyr(Y)363InsTer (nonsense)	X
35541	c.1107_1110del	p.Thr(T)369His(H)370InsTer (frameshift)	Meimaridou et al., 2012
265840	c.1163A>C	p.Tyr(Y)388Ser(S) (missense)	Hershkovitz et al., 2015
218365	c.1259dupG	p.His(H)421Ser(S)fs*4 (frameshift)	Jazayeri et al., 2015
2112825	c.1356_1357del	p.Lys(K)453fs (frameshift)	Meimaridou et al., 2012 Novoselova et al., 2015
35538	c.1598C>T	p.Ala(A)533Val(V) (missense)	Meimaridou et al., 2012
1119993	c.2274del	p.Ile(I)758fs (frameshift)	X
1705519	c.2635-1G>T	Splice acceptor variant	X
35540	c.2930T>C	p.Leu(L)977Pro(P) (missense)	Meimaridou et al, 2012
35543	c.3022G>C	p.Ala(A)1008Pro(P) (missense)	Meimaridou et al., 2012
265841	c.(−54 + 1_−53−1)_(381 + 1_382-1) del (*)	Exon 2 and 3 deletions	Roucher-Boulez et al., 2016
35542	c.3027T>G	p.Asn(N)1009Lys(K) (missense)	Meimaridou et al., 2012

Compiled using the ClinVar (www.ncbi.nlm.nih.gov/clinvar), OMIM (www.omim.org), and GeneCards (www.genecards.org) databases: only mutations from ClinVar currently classified as "pathogenic" and some to be classified as "likely pathogenic" were included. Protein indicates the protein including the mitochondrial targeting sequence (MTS; Fig. 2). Clinically, all mutations were associated with glucocorticoid deficiency 4, with or without mineralocorticoid deficiency (GCCD4; OMIM 614736). X, no reference available (ClinVar).

energized mitochondria is high, NNT-mediated NADPH production is favored, meaning that NNT is a key antioxidative enzyme (Rydstrom, 2006; Nickel et al., 2015). In this sense, the PMF allows maintaining the difference in redox state between the mitochondrial $NADP^+$/NADPH and NAD^+/NADH pools, although these have identical midpoint potentials (Rydstrom, 2006; Graf et al., 2021). The different redox states are directly linked to the biological roles of both pools (Murphy, 2015): (1) the mitochondrial NAD^+/NADH pool mainly serves to transport electrons from substrates to the ETC (Fig. 1D) and (2) the mitochondrial $NADP^+$/NADPH pool delivers electrons to GR and thioreductases (*e.g.,* TRXR2), thereby maintaining a high glutathione/oxidized glutathione (GSH/GSSG) ratio and reduced thioreductase levels (Fig. 1G; Murphy, 2012). As a consequence (Murphy, 2015), the mitochondrial $NADP^+$/NADPH pool is significantly more reduced (*i.e.,* its oxidation–reduction potential E_h equals ≈ -0.415V) than the NAD^+/NADH pool ($E_h \approx -0.300$V). Understanding NNT function and regulation requires quantitative information on the free concentrations of NADH, NAD^+, NADPH, and $NADP^+$ in the mitochondrial matrix. However, experimental quantification of these concentrations is challenging (*e.g.,* Sies et al., 2017). For instance, NADH, NAD^+, NADPH, and $NADP^+$ concentrations are not static but may change as a function of mitochondrial redox and metabolic state, especially during mitochondrial activation and/or pathological conditions. In addition, within cells these molecules are predominantly protein-bound (Xiao et al., 2018) and, in case of NADH and NADPH, their bound fractions apparently differ between tissues (Blacker et al., 2014). To complicate matters further, recent evidence suggests that the mitochondrial matrix fluid displays macromolecular crowding (Bulthuis et al., 2023), which may affect the (local) free concentration of NNT substrates. Analysis of total (*i.e.,* free + bound) metabolite concentrations in HeLa cells delivered estimated matrix concentrations for NADH ($\sim$8 μM), NAD^+ ($\sim$850 μM), and $NADP^+$ ($\sim$35 μM; Chen et al., 2016)). Although total NADPH levels were not reported in the latter study, application of the NADPH-detecting fluorescent sensor iNap3 reported a matrix-free NADPH concentration of $\sim$37 μM (Tao et al., 2017). The MIM is impermeable to NAD^+, NADH, NADPH, and $NADP^+$, requiring shuttle and transporter systems for their bidirectional transport (Xiao et al., 2018). In the case of mitochondrial [NADPH], evidence was provided that changes in this concentration are not paralleled by changes in cytosolic [NADPH] and *vice versa* (Niu et al., 2023). This physical and functional separation between NADPH pools is compatible with the fact that mitochondrial NADPH is not provided by the PPP (Fig. 1A), but instead generated by mitochondrial isocitrate dehydrogenase 1 (IDH1) and 2 (IDH2), malic enzyme 3 (ME3), mitochondrial 10-formyltetrahydrofolate dehydrogenase, and, more prominently, by NNT (Schiaffino et al., 2015; Vercesi et al., 2018; Kampjut and Sazanov 2019; Francisco et al., 2022). In this way, when mitochondrial ROS production is favored (*i.e.,* under conditions of high mitochondrial activity, high mitochondrial [NADH], and a highly negative $\Delta\psi$) also mitochondrial [NADPH] is increased by increased NNT action. This provides a mechanism that allows a better ROS removal under conditions of increased ROS production (Vercesi et al., 2018). The importance of NNT in this process is illustrated by the fact that: (1) the rate of mitochondrial NADPH-dependent H_2O_2 removal is greatly reduced in the absence of NNT activity (*e.g.,* Yin et al., 2012; Fisher-Wellman et al., 2016; Busanello et al., 2018; Francisco et al., 2018) and (2)

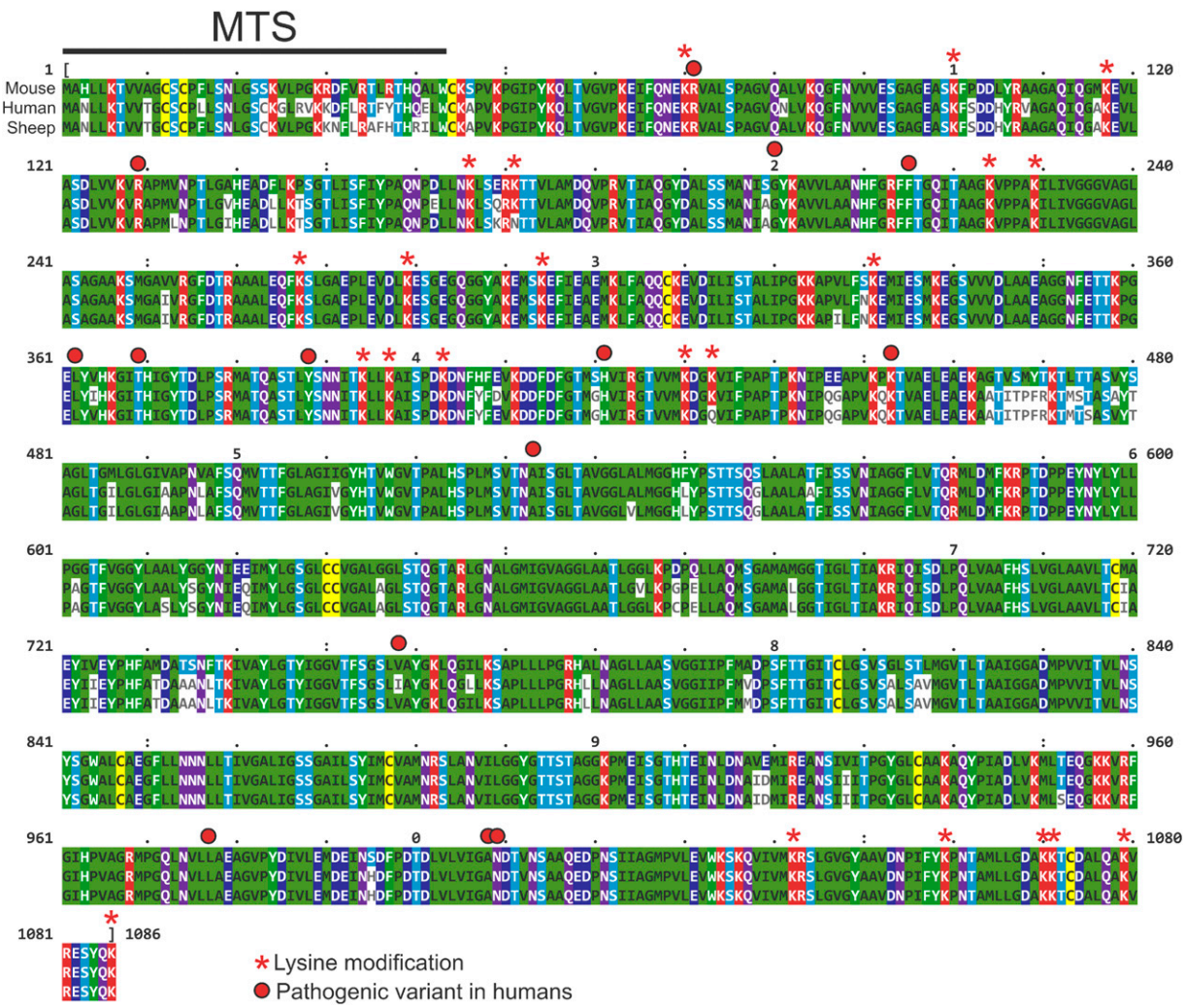

FIG. 4. NNT protein sequence, pathogenic mutations, and lysine modifications. NNT preprotein sequences for *Mus musculus* (Mouse; Q61941), *Homo Sapiens* (Human; Q13423), and *Ovis aries* (Sheep; W5PFI3) obtained from UniProt (www.uniprot.org). Sequences were aligned using EMBL-EBI tools (www.ebi.ac.uk) and visualized by Mview software (version 1.63; https://desmid.github.io/mview/). The percentage identity (PID) with the mouse sequence equaled 93.1% (human) and 93.5% (sheep). Pathogenic mutations in humans (red spheres; Table 1) and (predicted) lysine post-translational modifications (red asterisks; Table 2) are highlighted. This figure was compiled from (Huang et al., 2006; Meimaridou et al., 2013; Bainbridge et al., 2015; Roucher-Boulez et al., 2016).

NNT becomes the unique source of NADPH when the TCA cycle flux (including IDH2 flux) is inhibited during anoxia-like conditions (Ronchi et al., 2013; Ronchi et al., 2016).

NNT reverse-mode action

NNT can also operate in reverse. This is associated with NNT-mediated H^+ efflux from the mitochondrial matrix, NADH + $NADP^+$ production, and NADPH + NAD^+ consumption (Eq. I). NNT reverse-mode action was induced by a pathological workload increase in cardiac mitochondria during heart failure (HF), leading to increased NADH fueling of CI-linked ATP generation and a reduced NADPH-linked antioxidative capacity (Nickel et al., 2015). In contrast, when NNT was absent (*i.e.,* in C57BL/6J mice; see section "Impact of *Nnt* gene knockout in C57BL/6J mice"), the NADP/NADPH pool was maintained, and less oxidative damage was observed (Nickel et al., 2015). This strongly suggests that NNT in the heart can functionally switch from an antioxidant role (physiological workload) to a pro-oxidant role (pathological workload). NNT activity (measured in reverse mode) was 18% reduced in heart tissue biopsies from patients with end-stage chronic HF relative to nonfailing (NF) donor hearts (Sheeran et al., 2010), whereas NNT mRNA and protein levels were similar between HF and NF samples. HF tissues displayed lower total GSH (GSH+GSSG) amount, reduced GSH levels, and increased GSSG levels. GR activity, total NADPH content, total $NADP^+$ content, and NADPH/$NADP^+$ ratio were lower in HF than in NF samples. It was proposed that NNT function is impaired, potentially by oxidative damage, during severe HF in the mitochondrion-dense myocardium. This impairment was proposed to hamper the defense capacity of this tissue against oxidative insults (Sheeran et al., 2010). Compatible with this idea is the observation that mitochondrial ROS release was reduced in C57BL/6J relative to C57BL/6N ($Nnt^{+/+}$) mice, during the

transition of maladaptive right ventricular remodeling to right HF upon pressure overload (Müller et al., 2022). Analysis of pancreatic islets from C57BL/6J and C57BL/6N mice provided evidence that glucose treatment acutely increased the mitochondrial NADPH/$NADP^+$ ratio in an NNT-dependent manner (Santos et al., 2017). These phenomena were paralleled by a decreased NNT-dependent mitochondrial GSH oxidation, whereas cytosolic GSH oxidation was not greatly affected. Interestingly, this study implied the involvement of NNT reverse-mode action in the underlying mechanism, with NNT-mediated NADPH consumption being activated rather than NADPH production (forward mode). Comparative analysis of a control and cystic fibrosis (CF) cell model (human bronchial epithelial cell lines), revealed that higher NNT protein levels were paralleled by a lower NNT activity in CF cells, and that NNT runs in reverse mode in these cells (Favia and Atlante, 2021). Experiments with the *E. coli* transhydrogenase (EcTH) protein, reconstituted together with the *E. coli* F_oF_1-ATPase (CV) in liposomes, highlighted that NADPH-driven H^+-transport by reverse-mode EcTH action suffices to fuel ATP synthesis (Graf et al., 2021). Although the above insights on NNT reverse-mode action are highly relevant, understanding the NNT reverse-mode mechanism requires further study, for instance, in mice with conditional NNT deletion (Murphy, 2015) and/or other *in vitro* cell models.

Functional links between NNT and mitochondrial function

Under physiological conditions, NNT operates in the forward mode, in which the NNT-mediated consumption of NADH + $NADP^+$ and production of NAD^+ + NADPH is part of a PMF-dependent homeostatic mechanism (see section "NNT function and redox homeostasis"). In this sense, a negative $\Delta\psi$ can stimulate NNT activity, leading to increased mitochondrial NADPH formation, thereby enhancing mitochondrial antioxidant and reductase capabilities (Vercesi et al., 2018). In addition to PTM-linked mechanisms (see section "Post-translational modification of NNT"), NNT function also can (potentially) be regulated in other ways (Fig. 1) by the following: (1) (reversible?) formation of (active) NNT dimers from NNT monomers, (2) modulation of the PMF (*i.e.,* $\Delta\psi$, ΔpH), and (3) modulation of NNT substrate levels (NADH, $NADP^+$, NAD^+, NADPH). When in forward mode, NNT-mediated (NAD^+ + NADPH) generation consumes (NADH + $NADP^+$) and dissipates the PMF. Since both NADH (CI substrate) and the PMF are required for proper ETC functioning, it is expected that an altered NNT activity alters ETC function. As a consequence, this would affect ETC-linked ATP generation by CV, as well as various other $\Delta\psi$- or ΔpH-dependent mitochondrial processes. This suggests that changes in NNT activity, for example, could affect mitochondrial redox homeostasis, protein import, and the exchange of metabolites/ions between the cytosol and mitochondrial matrix (Fig. 1B–E, G). More directly, altered NNT function likely affects (local) NAD^+, NADH, $NADP^+$, and NADPH concentrations, thereby potentially altering (local) redox signaling (*e.g.,* Ying, 2008; Xiao et al., 2018; Yang et al., 2022). In this context, excessive levels of NADH, NADPH, and GSH induce "reductive stress," which can be equally harmful as oxidative stress (Xiao and Loscalzo, 2020; Yang et al., 2022). Functional cell/mitochondrial states that induce reductive stress by increasing the NADH/NAD^+ ratio include the use of CI exogenous substrates (*e.g.,* glutamate, malate [MAL]), hypoxia, NNT reverse-mode action, NNT inactivation (*e.g.,* loss-of-function mutations), and reverse-electron transfer (RET) to CI (*e.g.,* during ischemia-reperfusion). Reductive stress resulting from high NADH is also associated with elevated ROS production under ambient O_2 tensions (Xiao and Loscalzo, 2020). This occurs, for instance, *via* CI-mediated RET (Chenna et al., 2022) and by NADH-stimulated H_2O_2 formation by the TCA cycle enzyme α-KGDH (Tretter and Adam-Vizi, 2004). Regarding H_2O_2-linked ROS signaling, NNT was capable of sustaining NADPH-dependent H_2O_2 removal in intact skeletal muscle mitochondria (Figueira et al., 2021), and it was proposed that the CoQ10 pool and NNT action play a controlling role by affecting the rates of H_2O_2 production and degradation (Grayson & Mailloux, 2023). Mitochondria can take up Ca^{2+} from the cytosol *via* various mechanisms (Szabo and Szewczyk, 2023). When matrix Ca^{2+} levels become too high, the mitochondrial permeability transition pore (mPTP) is opened. Reversible (low conductance) "flickering" of the mPTP mediates the passage of Ca^{2+}, ROS, and H^+ downward of their concentration gradients. Extensive mPTP opening induces lasting $\Delta\psi$ depolarization, inhibition of ETC electron transport, loss of ATP, increased ROS generation, and mitochondrial swelling/rupture (Flores-Romero et al., 2023). NADP(H) redox changes are linked to mitochondrial Ca^{2+} release and mPTP opening (Vercesi et al., 2018), and NNT deficiency impairs mitochondrial redox homeostasis in such a way that Ca^{2+}-induced mPTP opening is facilitated (reviewed in Busanello et al., 2018). For instance, liver and heart mitochondria of C57BL/6J ($Nnt^{-/-}$) mice displayed increased ROS levels and a higher susceptibility to mPTP activation than C57BL/6JUnib ($Nnt^{+/+}$) mice (Salerno et al., 2019). Of note, increased ROS levels in $Nnt^{-/-}$ mice appear to be

FIG. 5. Evolutionary conservation of NNT amino acids. (A) Evolutionary conservation of the *Ovis aries* (sheep) NNT amino acid sequence (6QTI; www.rcsb.org) computed using the ConSurf server applying default settings (consurf.tau.ac.il; Ashkenazy et al., 2016). The extent of conservation ("ConSurf Grade") is color coded from blue (low conservation grade) to purple (high conservation grade). Amino acids for which insufficient data were available (marked yellow in panels B–F) were omitted. Functional NNT domains (defined using data from www.rcsb.org and Kampjut and Sazanov, 2019) are highlighted. **(B)** Visualization (front view) of amino acid conservation highlighted in one of the NNT monomers of the sheep NNT dimer. Sites for NAD^+ binding and proton translocated are indicated. **(C)** Same as panel B, but now depicting a 180° clockwise rotated version (along the vertical axis) of the dimer. The site for $NADP^+$ binding is indicated. **(D)** Same as panel B, but now depicting a 90° clockwise rotated version (along the vertical axis) of the NNT monomer. **(E)** Top view of panel B (marked "a"), highlighting the NAD^+ binding site. **(F)** Bottom view of panel B (marked "b"), highlighting the proton (H^+) entry site. NAD^+, oxidized form of nicotinamide adenine dinucleotide; $NADP^+$, oxidized form of nicotinamide adenine dinucleotide phosphate.

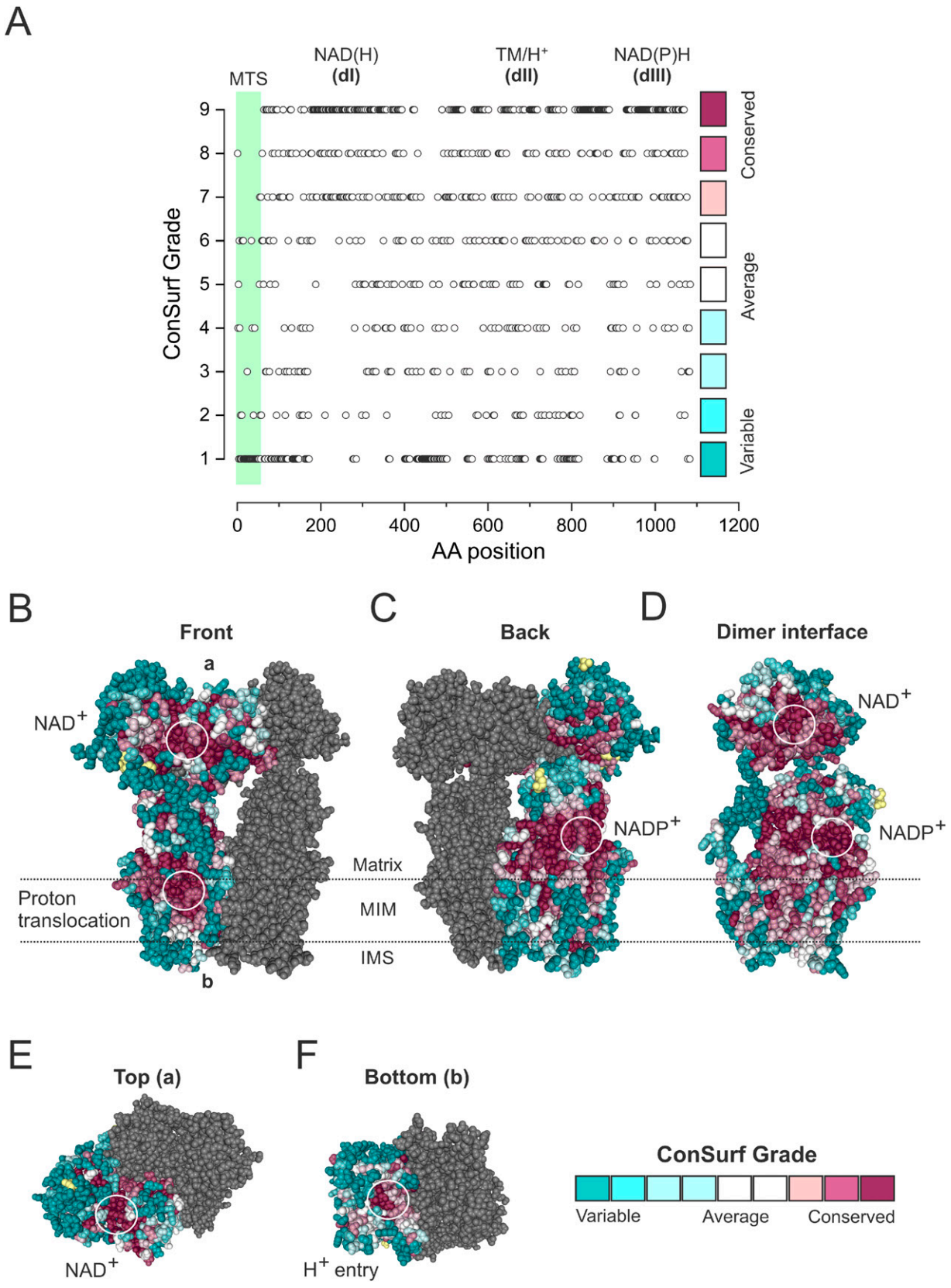

Table 2. Lysine Modifications of Nicotinamide Nucleotide Transhydrogenase in Human and Mouse

Species	*UniProt prediction*	*PLMD database*	*AA position (pre/mature)*		*Location in 3D structure (ovine)*	*Peptides (PLMD)*	*Type (UniProt and PLMD)*	*References (PLMD: PMID)*
Hs	X		70	27	dI, matrix		Acetylation	Predicted (UniProt)
Mm	X		70	27	dI, matrix		Acetylation	Predicted (UniProt)
Hs		X	100	57	dI, matrix	SGAGEAS**K**SDDHYR	Acetylation	Choudhary et al., 2009; Mertins et al., 2013; Wu et al., 2015; Svinkina et al., 2015; Zhu et al., 2016; Shen et al., 2016
Mm		X	100	57	dI, matrix	SGAGEAS**K**PDDLYR	Acetylation	Rardin et al., 2013; Nguyen et al., 2013
Mm		X	100	57	dI, matrix	SGAGEAS**K**PDDLYR	Succinylation	Boylston et al., 2015
Hs		X	117	74	dI, matrix	GAQIQGA**K**VLASDL	Acetylation	Sol et al., 2012; Weinert et al., 2013
Hs	X	X	117	74	dI, matrix	GAQIQGA**K**VLASDL	Succinylation	Weinert et al., 2013
Mm		X	117	74	dI, matrix	GAQIQGM**K**VLASDL	Acetylation	Fritz et al., 2012; Rardin et al., 2013; Park et al., 2013; Nguyen et al., 2013
Mm	X	X	117	74	dI, matrix	GAQIQGM**K**VLASDL	Succinylation	Park et al., 2013; Boylston et al., 2015
Hs		X	166	123	dI, matrix	QNPELLN**K**SQRKTT	Acetylation	Sol et al., 2012
Hs		X	171	128	dI, matrix	LNKLSQR**K**TVLAMD	Malonylation	Colak et al., 2015
Mm		X	171	128	dI, matrix	LNKLSER**K**TVLAMD	Acetylation	Park et al., 2013
Mm		X	171	128	dI, matrix	LNKLSER**K**TVLAMD	Succinylation	Park et al., 2013
Hs		X	224	181	dI, matrix	GQITAAG**K**PPAKIL	Acetylation	Svinkina et al., 2015
Hs	X		224	181	dI, matrix		Succinylation	Predicted (UniProt)
Mm		X	224	181	dI, matrix	GQITAAG**K**PPAKIL	Acetylation	Park et al., 2013
Mm	X	X	224	181	dI, matrix	GQITAAG**K**PPAKIL	Succinylation	Park et al., 2013
Mm		X	229	186	dI, matrix	AGKVPPA**K**LIVGGG	Acetylation	Rardin et al., 2013; Nguyen et al., 2013
Mm		X	229	186	dI, matrix	AGKVPPA**K**LIVGGG	Succinylation	Rardin et al., 2013; Boylston et al., 2015
Hs		X	267	224	dI, matrix	AAALEQF**K**LGAEPL	Ubiquitination	Sarraf et al., 2013
Mm		X	267	224	dI, matrix	AAALEQF**K**LGAEPL	Ubiquitination	Wagner et al., 2012
Hs		X	279	236	dI, matrix	EPLEVDL**K**SGEGQG	Ubiquitination	Sarraf et al., 2013
Hs		X	294	251	dI, matrix	GYAKEMS**K**FIEAEM	Acetylation	Zhu et al., 2016
Hs	X		294	251	dI, matrix		Succinylation	Predicted (UniProt)
Mm	X		294	251	dI, matrix		Succinylation	Predicted (UniProt)
Hs		X	331	288	dI, matrix	KAPVLFN**K**MIESMK	Acetylation	Choudhary et al., 2009
Hs	X		331	288	dI, matrix		Succinylation	Predicted (UniProt)
Mm	X		331	288	dI, matrix		Succinylation	Predicted (UniProt)
Hs		X	394	351	dI, matrix	LYSNNIT**K**LKAISP	Acetylation	Choudhary et al., 2009; Zhao et al., 2010; Sol et al., 2012; Weinert et al., 2013; Svinkina et al., 2015
Hs	X	X	397	354	dI, matrix	NNITKLL**K**ISPDKD	Acetylation	Choudhary et al., 2009; Beli et al., 2012
Mm	X		397	354	dI, matrix		Acetylation	Predicted (UniProt)
Hs		X	403	360	dI, matrix	LKAISPD**K**NFYFDV	Acetylation	Svinkina et al., 2015; Zhu et al., 2016
Hs		X	403	360	dI, matrix	LKAISPD**K**NFYFDV	Succinylation	Weinert et al., 2013
Hs		X	430	387	dI, matrix	IRGTVVM**K**GKVIFP	Succinylation	Weinert et al., 2013
Hs		X	433	390	dI, matrix	TVVMKDG**K**IFPAPT	Acetylation	Sol et al., 2012
Hs		X	1042	999	dIII, matrix	SKQVIVM**K**SLGVGY	Acetylation	Svinkina et al., 2015; Han et al., 2023
Mm		X	1059	1016	dIII, matrix	VDNPIFY**K**NTAMLL	Succinylation	Boylston et al., 2015
Hs		X	1070	1027	dIII, matrix	AMLLGDA**K**TCDALQ	Succinylation	Weinert et al., 2013
Mm		X	1070	1027	dIII, matrix	AMLLGDA**K**TCDALQ	Succinylation	Boylston et al., 2015

(*continued*)

TABLE 2. (CONTINUED)

Species	*UniProt prediction*	*PLMD database*	*AA position (pre/mature)*		*Location in 3D structure (ovine)*	*Peptides (PLMD)*	*Type (UniProt and PLMD)*	*References (PLMD: PMID)*
Hs		X	1071	1028	dIII, matrix	MLLGDAK**K**CDALQA	Acetylation	Mertins et al., 2013
Mm		X	1071	1028	dIII, matrix	MLLGDAK**K**CDALQA	Acetylation	Rardin et al., 2013; Park et al., 2013
Mm		X	1071	1028	dIII, matrix	MLLGDAK**K**CDALQA	Malonylation	Colak et al., 2015
Mm		X	1071	1028	dIII, matrix	MLLGDAK**K**CDALQA	Succinylation	Park et al., 2013; Boylston et al., 2015
Hs		X	1079	1036	dIII, matrix	TCDALQA**K**RESYQK	Acetylation	Svinkina et al., 2015
Hs	X		1079	1036	dIII, matrix		Succinylation	Predicted (UniProt)
Mm		X	1079	1036	dIII, matrix	TCDALQA**K**RESYQK	Acetylation	Rardin et al., 2013; Park et al., 2013
Mm	X	X	1079	1036	dIII, matrix	TCDALQA**K**RESYQK	Succinylation	Park et al., 2013
Mm		X	1079	1036	dIII, matrix	TCDALQA**K**RESYQK	Ubiquitination	Wagner et al., 2012
Mm		X	1086	1043	dIII, matrix	KVRESYQ**K**———	Succinylation	Boylston et al., 2015

Data compiled from: UniProt (www.uniprot.org) and the Protein Lysine Modification Database (PLMD 3.0; http://plmd.biocuckoo.org/). PLMD = experimental data. *Homo sapiens* (*Hs*; UniProt Q13423; PLMD-0017164). *Mus musculus* (*Mm*; UniProt Q61941; PLMD-0023832).
Modified amino acids are highlighted in bold.

particularly relevant during metabolic stress conditions [*e.g.,* in the presence of an additional low-density lipoprotein receptor mutation; (Salerno et al., 2019), or when receiving a high-fat diet (HFD; Navarro et al., 2017)].

NNT inhibitors

The availability of a specific and direct NNT-binding inhibitor would greatly facilitate functional studies. For example, palmityl-coenzyme A (palm-CoA; a.k.a. palmitoyl-coenzyme A) inhibited NNT function by competing with $NADP^+$ (Rydström, 1972) and was applied in later studies as an NNT inhibitor (*e.g.,* Lopert and Patel, 2014; Sharaf et al., 2017; Allouche et al., 2021). Unfortunately, palm-CoA also can inhibit the mitochondrial adenine nucleotide translocator, thereby directly affecting mitochondrial ATP/ADP exchange and bioenergetics (Ciapaite et al., 2006). Other presumed inhibitors also displayed effects not attributable to direct NNT inhibition. These included mitochondrial uncoupling, $\Delta\psi$ dissipation, stimulation of mitochondrial O_2 consumption, reduction of cell viability, and mPTP closure (Eriksson et al., 1998; Bicego et al., 2020). Taken together, we conclude that specific and directly NNT-binding inhibitors are currently lacking. However, *in silico* analysis of the NNT structure might prove useful in the discovery of such inhibitors (Kampjut and Sazanov, 2019).

NNT Gene Mutations and Disease in Humans

Pathogenic mutations in the human *NNT* gene (OMIM 607878; chromosome 5p12; Fig. 2) have been historically described in patients with unexplained glucocorticoid deficiency (GCCD) with or without mineralocorticoid deficiency (OMIM 614736; Table 1), originally classified as a member of the family of hereditary GCCD. GCCDs consist of typical adrenocorticotropic hormone (ACTH) resistance syndromes: (1) GCCD1 type 1 (mutations in the melanocortin 2 receptor [MCR2], a.k.a. adrenocorticotropic hormone receptor [ACTHR]), (2) GCCD2 (mutations in the melanocortin 2 receptor accessory protein [MRAP]), and (3) GCCD3 (other). All of these mutations induce dysfunction of the ACTH receptor, which impairs ACTH-induced stimulation of cortisol production in the adrenal cortex (*zona fasciculata*). However, in these forms of adrenal insufficiency, the renin–angiotensin–aldosterone system is still intact, allowing normal adrenal (*zona glomerulosa*) function, and no mineralocorticoid deficiency is observed. As a consequence, GCCD1, GCCD2, and GCCD3 display a selective GCCD with increased blood ACTH concentrations, which was previously classified as familial glucocorticoid deficiency (FGD). When left untreated, FGD is life-threatening due to the lack of cortisol and clinical features appear within the first months after birth (*i.e.,* failure to thrive, recurrent illnesses or infections, hypoglycemia, convulsions, shock; Meimaridou et al., 2012; Meimaridou et al., 2013; Yamaguchi et al., 2013; Fujisawa et al., 2015; Metherell et al., 2016; Roucher-Boulez et al., 2016; Krasovec et al., 2022; Li et al., 2022; Pons Fernández et al., 2024). Historically, *NNT* mutations were classified as GCCD4 because they were associated with high blood ACTH levels and cortisol deficiency. However, the underlying mechanism is completely different from the other three GCCDs (see section "Effect of *NNT*

mutations on adrenal function"), and GCCD4 is characterized by deficient mineralocorticoid production and a shortage of cortisol and aldosterone. *NNT* mutations account for <10% of the identified FGD cases where mutations in *MCR2* and *MRAP* were not observed (Maharaj et al., 2019). Analysis of a cohort of 23 patients with NNT-linked FGD demonstrated a median age of onset of 12 months (range: 3 days–39 months; Jazayeri et al., 2015). This study further reported no difference in age of disease onset between truncating and nontruncating *NNT* mutations. In contrast to the typical FGD-related features, a subset of patients also present, besides signs of cortisol deficiency, with symptoms of mineralocorticoid deficiency, such as weight loss, dehydration, and biochemical hyperkalemia (high K^+ blood levels) and hyponatremia (low Na^+ blood levels; Jazayeri et al., 2015; Weinberg-Shukron et al., 2015). Although most patients do not display cardiac disease symptoms (Maharaj et al., 2019), cardiac involvement was reported in case of biallelic *NNT* mutations (Roucher-Boulez et al., 2016), whereas heterozygous *NNT* loss-of-function mutations were associated with left ventricular noncompaction (Bainbridge et al., 2015). Recently, an interaction between the C-terminal tail of polycistin-1 (PC1 or PKD1) and NNT was demonstrated (Onuchic et al., 2023). Mutations in the PC1 gene induce autosomal dominant polycystic kidney disease. C-terminal PC1 cleavage products localized to mitochondria and suppressed the cystic phenotype and preserved renal function in an NNT-dependent manner (Onuchic et al., 2023).

Effect of NNT mutations on adrenal function

The mechanism that causes *NNT* mutation-linked adrenal dysfunction differs from the typical ACTH resistance syndromes that display a primary dysfunction of the ACTH receptor. Mitochondria in the adrenal cortex not only provide ATP but also harbor steroidogenic enzymes involved in mineralocorticoid and corticoid synthesis. In this sense, the cytochrome P450 (CYP) enzyme family, consisting of endoplasmic reticulum (ER)- and mitochondria-localized members, represents the majority of steroidogenic enzymes (Midzak and Papadopoulos, 2016). Interestingly, the CYP enzymes located in mitochondria (*e.g.,* CYP11A1; CYP11B1, CYP11B2; Hu et al., 2004; Miller, 2011) use an "ETC" consisting of ferredoxin reductase (FDXR; 54-kDa; *i.e.,* NADPH:adrenodoxin oxidoreductase) and ferredoxin 1 (FDX1; 14-kDa; *i.e.,* adrenodoxin). This chain mediates electron transfer from NADPH. In this system, electrons are transported one by one by the mobile transporter FDX1 to CYP (Fig. 6). The latter enzyme then catalyzes the first step of mineralocorticoid and corticoid synthesis. NNT-mediated NADPH production plays a key role in this mechanism (Bodoni et al., 2023).

Pathomechanism of NNT mutations

Many of the initially reported *NNT* mutations were nonsense and/or frameshift mutations, probably leading to premature truncation of the protein (Meimaridou et al., 2012). This suggests that patients with *NNT* mutations, similar to C57BL/6J mice (see section "Impact of *Nnt* gene knockout in C57BL/6J mice"), do not express NNT protein. However, the mutation-reporting studies generally presented no

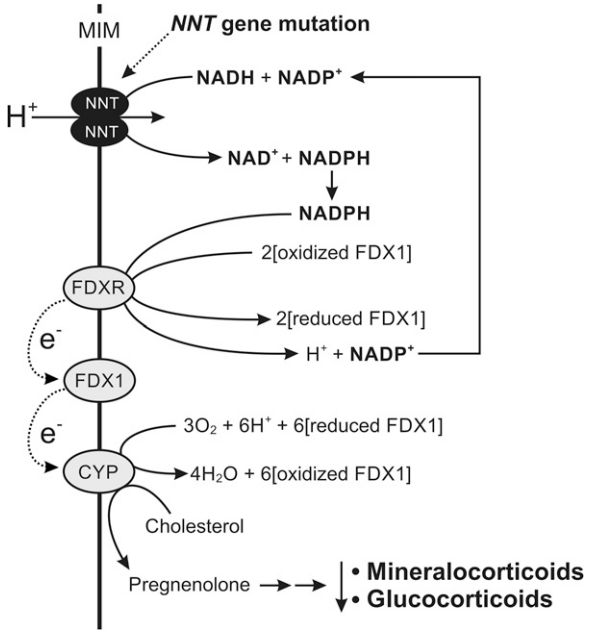

FIG. 6. Adrenal pathomechanism in GCCD4 patients carrying *NNT* gene mutations. This scheme illustrates how NNT dysfunction affects mineralocorticoid and glucocorticoid synthesis in human patients. NNT activity recycles $NADP^+$ to NADPH, from which electrons (e-) are abstracted by FDXR and subsequently transported to FDX1 and CYP. The latter enzyme then catalyzes the first and rate-limiting step of mineralocorticoid and corticoid synthesis. See main text for details. CYP, cytochrome P450; FDXR, ferredoxin reductase; NADPH, reduced form of nicotinamide adenine dinucleotide phosphate.

experimental data (*e.g.,* using Western blotting) on NNT protein levels in patient-derived cells/tissues (Meimaridou et al., 2012; Meimaridou et al., 2013; Yamaguchi et al., 2013; Bainbridge et al., 2015; Fujisawa et al., 2015; Hershkovitz et al., 2015; Jazayeri et al., 2015; Novoselova et al., 2015; Weinberg-Shukron et al., 2015; Roucher-Boulez et al., 2016; Krasovec et al., 2022; Li et al., 2022; Bodoni et al., 2023; Pons Fernández et al., 2024). This prevents a detailed understanding of the pathomechanism (*e.g.,* are the reported *NNT* mutations exerting their pathogenic effects *via* NNT catalytic impairment and/or *via* lowering NNT protein levels?), and complicates translational comparison between human NNT patients and C57BL/6J mice. However, recent analysis of patient peripheral blood mononuclear cells (PBMCs) demonstrated reduced NNT protein levels and undetectably low (*i.e.,* <4% of control) NNT activity (measured as reverse activity; Francisco et al., 2024). These patients ($n = 5$; mean age: 12.5 years) suffered from primary adrenal insufficiency and harbored novel homozygous NNT variants (exon 12 and 14 deletions, c.259C>T, c.764G>A, c.1109A>G, c.2507G>A). The absence of NNT reverse-mode activity did not correlate with citrate synthase (CS) activity, suggesting that the NNT mutations did not affect mitochondrial content. In healthy heterozygous carriers (*i.e.,* parents of the patients; $n = 8$; mean age = 39.6 years), average NNT reverse-mode activity equaled 49% of control values. This suggests that the NNT reverse-mode activity decrease is gene-dose dependent. NNT reverse-mode activity normalized to CS

was not correlated with age or gender in the healthy control group ($n = 19$; mean age: 33.5 years). NNT protein expression was reduced to 61% in carriers. In four patients, NNT protein was present at low levels or not detectable at all. In contrast, NNT protein levels were normal for the c.2507G>A mutation (Francisco et al., 2024). In patient PBMCs, NNT mRNA expression levels did not correlate with mature protein expression, whereas carriers displayed mRNA expression levels similar to controls. Analysis of mitochondrial O_2 consumption in permeabilized PBMCs of three patients (c.764G>A, c.1109A>G, c.2507G>A) did not reveal significant differences with controls (Francisco et al., 2024).

In another study, analysis of lymphocyte-derived mitochondria-enriched fractions of a homozygous patient (c.644T>C mutation), yielded an NNT-specific activity equaling 31% of the mean control value (Fujisawa et al., 2015). In comparison, the (heterozygous) parents of this patients displayed a 61% NNT-specific activity, again suggesting that the NNT activity decrease is gene-dose dependent. Although this study did not determine NNT protein levels, the detection of a reduced NNT activity in the patient lymphocytes strongly suggests the presence of less (fully functional) NNT protein, normal NNT protein amounts with a reduced activity, and/or a combination of the two. Patient lymphocyte mitochondria also displayed increased protein nitration, potentially indicative of nitrative stress, and a reduced mtDNA copy number and mitochondrial mass (Fujisawa et al., 2015). Relative to control, CS activity was 70–80% lower in patient cells and heterozygous carriers (parents). CIV activity (normalized to CS) was similar between carriers and controls, but lower in patient's lymphocytes.

Analysis of the homozygous *NNT* variant p.G866D (gene mutation not reported) revealed normal *NNT* mRNA expression in mononuclear peripheral blood cells (Bodoni et al., 2023). Relative to control, *NNT*-mutated cells displayed increased ROS levels, which were further increased by exogenous H_2O_2 addition. The latter was not observed in control cells. GSH levels were lower in the patient cells, relative to control and heterozygous carriers. Following exogenous H_2O_2 application, GSH levels were decreased in the following order: patient > carrier > control. The ATP content and viability of the patient cells were normal under basal conditions but significantly decreased after exogenous H_2O_2 application. Mitochondrial mass was reduced in the patient cells relative to controls and this difference increased following exogenous H_2O_2 application.

In case of the c.598G>A mutation, patient skin fibroblasts exhibited increased ROS levels, decreased ATP content, and a fragmented mitochondrial structure (Weinberg-Shukron et al., 2015).

For three presumably pathogenic *NNT* mutations (c.811G>A, c.2078G>A, and c.2581G>A), NNT protein levels on Western blot were reduced relative to control (Li et al., 2022). However, these levels were not determined in patient-derived cells but in nthy-ori 3.1 cells, transiently transfected with plasmids encoding normal and mutated NNT variants. This revealed that mutated NNTs were less overexpressed than normal NNTs, although their mRNA levels were similar, suggesting that the mutated NNT proteins are destabilized. In the same nthy-ori 3.1 cell model, total NADPH/$NADP^+$ increased less in cells overexpressing mutated NNT variants than in cells overexpressing normal NNT (Li et al., 2022). This might suggest that the highlighted mutations impair NNT function *via* lowering NNT protein levels.

We conclude that for the majority of reported *NNT* mutations, it is still unclear whether they induce pathology by impairing NNT catalytic function and/or reducing NNT protein levels. In this context, a recently presented cell-reprogramming based adrenal model might be of great value to study the pathomechanism of specific NNT mutations within an isogenic background (Sakata et al., 2022).

Impact of *Nnt* Gene Mutations in C57BL/6J Mice

The most widely used "WT" mouse inbred strain (C57BL/6J), derived from the original C57BL strain in 1948, harbors a missense mutation in exon 1 (M35T) and a deletion of exons 7–11 in the *Nnt* gene (Fig. 2; Toye et al., 2005; Huang et al., 2006; Mekada and Joshiki, 2009; Figueira, 2013; Kraev, 2014; Goldstein and Wagers, 2018). As a consequence, the NNT protein is absent, as demonstrated by Western blot analysis of liver, brain, kidney, heart, and macrophages (Huang et al., 2006; Parker et al., 2009; Usami et al., 2018; Salerno et al., 2019; Williams et al., 2021; Dogar et al., 2020). However, when compared with the C57BL/6N "WT" strain, C57BL/6J mice exhibit >200 identified sequence variations and various phenotypic differences (Timmermans and Libert, 2018; see: www.jax.org for a complete overview). These differences potentially impact upon the penetrance and expression of mutational effects in these strains (Simon et al., 2013). For instance, C57BL/6J mice are homozygous for $Cdh23^{ahl}$ (age-related hearing loss 1 mutation), resulting in the onset of progressive hearing loss at 10 months of age. Being both derived from C57BL/6 inbred mice C57BL/6J ($Nnt^{-/-}$) and C57BL/6N ($Nnt^{+/+}$), these animals have often been compared solely for this NNT difference. However, phenotypic differences between these substrains cannot be solely explained by *Nnt* gene mutations (Nemoto et al., 2022). This discrepancy between *Nnt* genotypes, as well as its potential impact on other genetic backgrounds (*e.g.,* mtSOD-deficient mice, Bcl2l2-mutated mice), can complicate interstudy comparisons of knockout mouse studies (*e.g.,* Huang et al., 2006; Kim et al., 2010; Navarro et al., 2012; Williams et al., 2020; Rawle et al., 2022). Below we describe how the mouse *Nnt* gene mutation affects specific organs and systemic functions.

Adrenal gland

Comparative analysis of the adrenal glands from C57BL/6J (control) and C57BL/6J (*Nnt*-mutated) revealed a slight disorganization of *zona fasciculata* and higher levels of apoptosis in the latter animals (Meimaridou et al., 2012). A later study extended these observations by demonstrating that *Nnt* deficiency did not affect the mRNA levels of CYP11A1, the enzyme responsible for the first step in steroidogenesis, but significantly reduced the protein content of CYP11A1 and various antioxidant enzymes (TXNRD2, PRDX3, GPX1; Meimaridou et al., 2018). In a preliminary study, we observed that the CYP11A1 protein content is also significantly reduced in the testis of C57BL/6J mice (K.J. Teerds, unpublished observation). Transcriptome analysis revealed that loss of NNT was associated with increased expression

of OXPHOS complexes, TCA cycle, and sugar metabolism mRNA in C57BL/6J adrenal and hearts (Williams et al., 2021). Interestingly, the latter study also examined a mouse model (C57BL/6J-BAC) expressing the full-length *Nnt* gene on the C57BL/6J background. Surprisingly, a comparative analysis of three tissues with a relatively high metabolic demand (adrenal, testis, heart) revealed only minor differences between C57BL/6J and C57BL/6J-BAC. It was hypothesized that other background variants might be relevant in regulating the transcriptome and phenotypes of these mice (Williams et al., 2021).

Brain

NNT expression is unevenly distributed across brain regions and its loss affects responses to acute psychological stress and induces depressive-like behavior and motor dysfunction (Picard et al., 2015; Francisco et al., 2020). During migraine, cortical spreading depression causes an initial severe drop in NADH levels, leading to NNT-mediated impairment of antioxidant defense systems (reviewed in Borkum, 2021). Comparison of cerebellar mitochondria isolated from C57BL/6J and C57BL/6N mice revealed a lower mitochondrial mass (CS activity), lower CI, CIV, and CV activities (normalized on CS), and a reduced mtDNA copy number (Fujisawa et al., 2015). Concerning the cerebellum, it was further proposed that the stability of cerebral vessel walls in very young mice might be reduced by NNT absence and the ensuing increased oxidative stress (Wolf et al., 2016). Brain cortex mitochondria from C57BUnib.B6-*Nnt*$^{-/-}$ mice displayed no detectable NNT activity in comparison with C57BUnib.B6-*Nnt*$^{+/+}$ (control) mice (Francisco et al., 2018). Relative to other NADPH-producing enzymes (*e.g.,* IDH2, MEs, and GDH), NNT activity represented 26% of the total activity in young (4 months) and old (19 months) *Nnt*$^{-/-}$ and control mice. Furthermore, NNT, IDH2, and ME3 were identified as the primary sources of NADPH. Mitochondrial mass (CS activity) did not differ between C57BUnib.B6-*Nnt*$^{-/-}$ and C57BUnib.B6-*Nnt*$^{+/+}$ mice (Francisco et al., 2018). Interestingly, whole-brain analysis revealed that nonsynaptic mitochondria exhibited a higher NNT activity than synaptic mitochondria. *Nnt*$^{-/-}$ mitochondria further displayed hampered $NADP^+$ reduction, impaired H_2O_2 removal, and increased H_2O_2 release. The latter, for instance, occurred during CI inhibition. These results illustrate that brain cortex mitochondria with impaired NNT function display a deficient H_2O_2 removal.

Heart

Analysis of NNT activity in heart mitochondria of C57BL/6J mice demonstrated that NNT enzymatic activity was $\sim$2% of that detected in control (C57BL/6Junib) mice (Ronchi et al., 2013). Loss of NNT function in C57BL/6J mice has been shown to have a close relationship with cardiometabolic alterations (*e.g.,* HF). HF is associated with a functional block of CI and increased $O_2^{\bullet-}$ and H_2O_2 production. TCA cycle-derived NADH is used as a CI substrate and for NNT-mediated H_2O_2 removal (Wagner et al., 2020). Previous evidence suggests that NADH can stimulate H_2O_2 formation by the TCA cycle enzyme α-KGDH (Tretter and Adam-Vizi, 2004). Cardiac mitochondria of C567BL/6J mice released more H_2O_2 using α-KG as a substrate than using pyruvate/MAL as substrates. This release was stimulated further by the CI inhibitor rotenone. In contrast, H_2O_2 release was equally low in C567BL/6N cardiac mitochondria with α-KG and pyruvate/MAL as substrates (Wagner et al., 2020). Mechanistically, it was concluded that α-KGDH generates NADH for NNT-mediated NADPH formation and not for CI-mediated electron transport (see section "Brain"). This suggests that in the heart: (1) α-KGDH is important for H_2O_2 removal but not for $O_2^{\bullet-}$ production, and (2) during HF, CI-linked oxidative stress is mitigated by α-KGDH/NNT-dependent NADPH formation (Wagner et al., 2020). Alternatively, NNT might run in reverse mode during HF (see section "NNT reverse-mode action"). Comparison of C57BL/6J, C57BL/6J, and transgenic animals in which the *Nnt* mutation was rescued (C57BL/6J-BAC mice) at 3, 12, and 18 months of age highlighted a minor dilated cardiomyopathy (CM) in C57BL/6J mice (Williams et al., 2020). The latter was accompanied by sarcomere organization defects and eccentric hypertrophy. Importantly, it was found that C57BL/6J mice harbor a mutation in myosin light chain kinase (*Mylk3*), leading to the absence of MYLK3 protein. This suggests that the *Mylk3* mutation is responsible for the modest CM phenotype in C57BL/6J mice (Williams et al., 2020).

Muscle

In skeletal muscle mitochondria with low NNT activity, α-KGDH is a major source of $O_2^{\bullet-}$ and H_2O_2 at high NADH levels (Wagner et al., 2020). Using skeletal muscle tissue and mitochondria from C57BL/6N and C57BL/6J mice, an effort was made to determine the interplay between mitochondrial NNT and ETC activities (Smith et al., 2020). To this end, it was investigated how increased mitochondrial ROS (H_2O_2) production during conditions of high substrate oxidation (resting state) is counterbalanced by increased O_2 consumption due to elevated NNT-mediated mitochondrial proton influx. The obtained results suggest that, under these conditions, GSH and TRXRs (Fig. 1G) use NNT-generated NADPH, and that the latter is produced using the ETC-sustained PMF (Smith et al., 2020; Kaludercic and Di Lisa, 2020). Quantitatively, ETC-mediated O_2 consumption was 18.6% lower in C57BL/6J mice, supporting the conclusion that mitochondrial respiration supports NNT activity to allow optimal ROS removal. However, these findings were subsequently challenged (Figueira et al., 2021) and it was concluded that more direct evidence is required to define the quantitative contribution of NNT-linked redox circuits to energy expenditure *in vivo* (Smith et al., 2021).

Liver

Analysis of isolated heart mitochondria from C57BL/6J mice demonstrated no detectable NNT activity (Ronchi et al., 2013). Comparison with C57BL/6Junib mice (an *Nnt* WT mouse strain) revealed that C57BL/6J mice display the following: (1) normal maximal IDH2 activity, (2) a lower GSH/GSSG ratio, (3) similar total glutathione (GSH+GSSG) levels, (4) similar mitochondrial O_2 consumption when respiring on CI- or CII-linked substrates, (5) a higher rate of H_2O_2 release when respiring on CII-substrates (succinate + rotenone condition), but not on CI substrates (pyruvate + MAL condition), (6) spontaneous NADPH oxidation in the absence of endogenous TCA cycle substrates, and (7) an

increased susceptibility for Ca^{2+}-induced mPTP opening (Ronchi et al., 2013).

Interestingly, liver mitochondria of C57BL/6J mice displayed ~7.7-fold higher catalase (CAT) protein levels relative to C57BL/6NJ mice (Dogar et al., 2020). The latter is a sub-line of C57BL/6, which does not exhibit the *Nnt* gene deletion. CAT is an antioxidant enzyme mediating the conversion of H_2O_2 into H_2O, typically not expressed in mitochondria. Liver mitochondria are an exception to this rule (Salvi et al., 2007). C57BL/6J and C57BL/6NJ mitochondria generated H_2O_2 at similar rates using pyruvate as a substrate, whereas H_2O_2 production was higher in C57BL/6J mitochondrial pyruvate or succinate displayed similar rates of H_2O_2 removal, it was concluded that CAT upregulation in C57BL/6J mitochondria serves to maintain H_2O_2 steady-state levels. In contrast, liver mitochondria from C57BL/6NJ mice depended more on GSH- and TRX-linked systems for clearance of exogenous H_2O_2 (Dogar et al., 2020). These findings are consistent with a mechanism in which CAT upregulation compensates for the loss in NNT-mediated H_2O_2-removal capacity in C57BL/6J liver mitochondria. However, it is likely that the relative contribution of NNT to NADPH-dependent mitochondrial H_2O_2 removal is codetermined by the respiratory state of the mitochondrion and/or substrates that sustain its energy metabolism (Ronchi et al., 2016).

As a model of non-alcoholic fatty liver disease (NAFLD), also referred to as metabolic dysfunction-associated fatty liver disease, C57Unib.B6 congenic mice with ($Nnt^{+/+}$) or without ($Nnt^{-/-}$) NNT activity were subjected to a HFD (60% of total calories [en%]; Navarro et al., 2017). After 20 weeks, relative to $Nnt^{+/+}$ animals, $Nnt^{-/-}$ mice displayed a higher content of liver triglycerides, increased prevalence of steatohepatitis, higher mitochondrial H_2O_2 release, decreased aconitase activity, and increased susceptibility to Ca^{2+}-induced mPTP opening. The diet also stimulated PDH phosphorylation (leading to PDH inhibition) and reduced the H_2O_2 removal capacity in $Nnt^{-/-}$ mice. These data are compatible with NNT preventing mitochondrial redox imbalance, PDH inhibition, and NAFLD progress. A follow-up study demonstrated that the HFD reduced the ability of isolated $Nnt^{-/-}$ liver mitochondria to remove H_2O_2, and that this reduction was prevented by dichloroacetate (DCA; Navarro et al., 2022). DCA decreased PDH phosphorylation levels in the liver and also prevented NAFLD aggravation in $Nnt^{-/-}$ mice on an HFD. Although some toxic effects were observed, these results suggest that DCA might protect against NAFLD in $Nnt^{-/-}$ mice by preventing PDH inactivation, thereby allowing liver mitochondria to remove H_2O_2 in a pyruvate-supported manner (Navarro et al., 2022). Compatible with this idea, a comparative analysis of *M. gastrocnemius* muscle from C57BL/6N and C57BL/6J mice suggested the existence of a $\Delta\psi$-dependent redox circuit connecting the pyruvate dehydrogenase complex (PDHC) and NNT (Fisher-Wellman et al., 2015). In this mechanism, PDHC-produced H_2O_2 is removed by the GR/TRX system (Fig. 1G), which is sustained *via* NNT-generated NADPH, at the expense of NADH (CI substrate) and $\Delta\psi$. In this way, NNT-linked "energy expenditure" is linked to PDHC-linked metabolic pathways, potentially explaining why C57BL/6J mice display a lower energy expenditure and are more susceptible to diet-induced obesity (Fisher-Wellman et al., 2015).

Kidney

In an experimental model of kidney stone formation, calcium oxalate crystal deposition in the kidneys of C57BL/6J mice was higher than in C57BL/6N mice. This might indicate that the absence of *NNT* protein stimulates crystal formation in C57BL/6J mice (Usami et al., 2018).

Hyperpigmentation

Compatible with the observed hyperpigmentation in FGD patients (see section "*NNT* gene mutations and disease in humans"), increased fur pigmentation (eumelanin) was also observed in C57BL/6J mice relative to C57BL/6NJ mice (Allouche et al., 2021). A distinct NNT- and ROS-dependent pigmentation mechanism was proposed (*i.e.,* independent of the established UVB-cAMP-MITF tanning pathway), in which pigmentation in cells of melanocytic origin is affected by oxidative stress.

Glucose homeostasis and obesity

C57BL/6J mice display a reduced glucose tolerance for which NNT absence was proposed to be responsible (Toye et al., 2005; Parker et al., 2009; Salerno et al., 2019). Supporting this conclusion, introducing a functional NNT into C57BL/6J mice rescued impaired insulin secretion and glucose intolerance (Freeman et al., 2006). Analysis of glucose-stimulated insulin secretion (GSIS), insulin sensitivity, clearance, and central glucose-induced insulin secretion (Fergusson et al., 2014), demonstrated that C57BL/6J mice display the following: (1) impaired GSIS upon glucose administration intravenously (tolerance test and hyperglycemic clamp), (2) no impaired GSIS upon oral glucose administration, and (3) no change in body insulin sensitivity, insulin clearance, β cell mass, or central response to glucose. It was concluded that C57BL/6J mice exhibit defective β cell function and insulin secretion (Fergusson et al., 2014). In contrast, another study provided evidence that the *Nnt* mutation does not affect insulin secretion and glucose tolerance (Wong et al., 2010). Moreover, using the streptozotocin (STZ)/nicotinamide (NA)-induced diabetes model, blood glucose and plasma insulin levels were lower in C57BL/6J mice relative to the ICR (Institute of Cancer Research) strain mice (Shimizu et al., 2012). Similarly, a comparative analysis of C57BL/6J and C57BL/6N mice suggested that a lack of functional NNT only moderately affects GSIS and glucose tolerance (Close et al., 2021). Analysis of human visceral and subcutaneous adipose tissue samples (221 subjects) demonstrated that visceral NNT mRNA expression is higher in obese patients (Heiker et al., 2013). Moreover, this expression correlated with body weight, body mass index, % body fat, visceral/subcutaneous fat area, waist/hip circumference, and fasting plasma insulin levels. This suggests that NNT is functionally relevant in the development of human obesity. The C57BL/6J male mouse model is widely used as a control strain in diet-induced obesity (DIO) studies (*e.g.,* Surwit et al., 1988; Nicholson et al., 2010; Fisher-Wellman et al., 2016; Kunath et al., 2020). Comparison of the time-dependent metabolic responses to a high-fat/high-sucrose

diet revealed that both C57BL/6J and C57BL/6NJ mice displayed an impaired glucose tolerance within 24 h after the start of the diet (Fisher-Wellman et al., 2016). Moreover, marker levels of the metabolic syndrome and H_2O_2-induced stress were reduced in C57BL/6J animals, probably due to compensatory responses in non-NNT-related homeostatic redox pathways. These findings suggest that a high-fat/high-sucrose diet similarly impacts on C57BL/6J and C57BL/6NJ mice (Fisher-Wellman et al., 2016). In contrast, C57BL/6J mice on an HFD (45en%) displayed obesity, hyperinsulinemia, elevated basal serum insulin levels, mildly elevated blood glucose levels, a blunted GSIS, and increased pancreatic islet mass/size (Roat et al., 2014). The latter study also demonstrated that pancreatic islets from HFD animals displayed an elevated O_2 consumption rate (OCR), which was not stimulated by glucose or the mitochondrial uncoupler carbonyl cyanide-4-trifluoromethoxyphenylhydrazone (FCCP). Similarly, comparative analysis of male C57BL/6J and C57BL/6NJ mice during 14 weeks of HFD (60en%) revealed that both strains were DIO-sensitive and displayed a similar weight at 6 weeks (Nicholson et al., 2010). C57BL/6J males presented with a (3 g) higher weight at 20 weeks. The latter was accompanied by increases in both lean and fat mass. Regarding glucose homeostasis, C57BL/6J male mice displayed higher nonfasting glucose levels and an impaired glucose tolerance at 8 and 20 weeks. This was paralleled by increased levels of leptin in the serum, whereas insulin levels were not affected. When placed on a lower-fat diet (10en%), C57BL/6J male mice displayed lower serum 0.01w?>insulin levels and weight gain relative to C57BL/6NJ mice (Nicholson et al., 2010). Another DIO study used first backcross (BC1) hybrids of WT *Nnt* expressing C57BL/6NTac and *Nnt*-mutant C57BL/6JRj mice [(C57BL/6NTac × C57BL/6JRj)F1 × C57BL/6NTac] (Kunath et al., 2020). Both male and female BC1 hybrid animals were analyzed for weight gain and specific fat-pad depot mass under HFD conditions (58en%). Similar to C57BL/6J male mice (Nicholson et al., 2010), both male and female BC1 animals displayed a reduction in weight gain, relative epididymal fat mass, and relative subcutaneous fat mass, relative to WT animals (Kunath et al., 2020).

Aging

Aging has been linked to a large number of molecular changes, including those at the level of the (epi)genome, immune system, and mitochondria. However, it is still unclear how aging is brought about and whether changes are causative or epiphenomenal (de Magalhães, 2024). In this sense, NADPH levels decline during aging in several tissues, but it is still unclear whether this drop is relevant to the aging process (Bradshaw, 2019). Aging is a major risk factor in Alzheimer's disease (AD) and has been linked to aberrant redox homeostasis, increased ROS generation, and mitochondrial dysfunction (Ghosh et al., 2014). Analysis of AD neuronal models revealed that NAD(P)H or GSH depletion correlated linearly with cell death. Interestingly, gene expression of key redox enzymes, including NNT, decreased in an age-dependent manner and apparently contributed to the age-related decline in NAD(P)H levels. Taken together, the above suggests that NAD(P)H exerts upstream control of GSH and ROS levels (Ghosh et al., 2014) and that the parallel age-dependent decline in NNT and NADPH levels might somehow be linked to the aging process. Concerning NAD^+, recent evidence suggests that RET at CI, causing increased ROS generation and increased conversion of NAD^+ into NADH (thereby increasing NADH/NAD^+ ratio), is active during aging (Rimal et al., 2023). Also in mitochondrial diseases, an increased NADH/NAD^+ ratio is likely to be part of the pathomechanism (*e.g.,* Katsyuba et al., 2020; Chini et al., 2021). Regarding NNT, it was proposed that the NADH/NAD^+ ratio can be normalized by NNT activation or overexpression (Olgun, 2009). In this sense, it was presented that mtDNA mutations that increase ROS levels in the presence of functional NNT were associated with an increased health span in mice (Hirose et al., 2016; Latorre-Pellicer et al., 2016). To the best of our knowledge, there is no comprehensive tissue-wide information yet on the aging process in $Nnt^{-/-}$ mice, but this model provides a great opportunity to study this process in the context of NNT-linked NAD(P)H homeostasis and mitochondrial bioenergetics. In this sense, a recent study comparatively analyzed motor performance and skeletal muscle bioenergetic function in young, middle-aged, and older NNT-deficient mice (Navarro et al., 2024). These animals were subjected to a wire-hang test (locomotor performance), which yielded a decreased score for middle-aged and older NNT-deficient mice, relative to age-matched controls. Similarly, skeletal muscle samples of middle-aged/older mice (soleus and vastus lateralis) exhibited a reduced O_2 consumption (Navarro et al., 2024). It was concluded that declining NNT expression induces locomotor impairments and muscle dysfunction in aging mice.

Immune system

Comparative analysis of C57BL/6J mice and C57BL/6J-NNT mice (in which the *Nnt* mutation was rescued by transgenic expression of the entire *Nnt* gene) revealed that C57BL/6J mice are more resistant to pulmonary infection with *S. pneumonia* than C57BL/6J-NNT mice (Ripoll et al., 2012). Moreover, relative to C57BL/6J-NNT mice: (1) C57BL/6J animals induced a stronger inflammatory response, (2) C57BL/6J macrophages generated more ROS, nitric oxide (NO), and proinflammatory cytokines in response to *S. pneumonia*, and (3) C57BL/6J macrophages are less resistant to *S. pneumonia*-induced apoptosis. These results suggest that NNT is important in the regulation of macrophage-mediated inflammatory responses (Ripoll et al., 2012).

Hematopoietic stem cells

Hematopoietic stem and progenitor cells (HSPCs) are exposed to considerable oxidative stress during hematopoietic stem cell transplantation (Mantel et al., 2015). Comparative analysis of HSPC function between C57BL/6N and C57BL/6J mice revealed that the latter displayed a compromised short-term hematopoietic repopulating activity (Morales-Hernandez et al., 2018). Moreover, HSPCs from C57BL/6J animals displayed higher ROS levels and were more sensitive to exogenously induced oxidative stress. It is likely that the observed aberrations are primarily due to NNT absence, since they were mimicked by NNT knockdown in C57BL/6N-derived HSPCs (Morales-Hernandez et al., 2018).

Atherosclerosis

Mitochondrion-derived ROS play an important role during inflammation and vascular remodeling linked to the formation of atherosclerotic plaques (Vozenilek et al., 2018). When subjected to an HFD (~35–40 en%), basic vascular ROS levels increased in both C57BL/6N and C57BL/6J mice, but where higher in the latter. This HFD-induced ROS increase was fully prevented by cotreatment with the mitochondria-targeted antioxidant MitoTEMPO (an SOD mimetic), which reduced the elevated vascular ROS levels to a similar extent in C57BL/6N and C57BL/6J mice (Vozenilek et al., 2018). With respect to HFD-induced atherosclerotic plaque formation, C57BL/6J animals displayed a higher atherosclerotic burden (aortic arch and whole aorta) than C57BL/6N mice. In line with its function as a mitochondrial redox balance regulator, these findings suggest that NNT loss can contribute to enhanced cardiovascular pathologies (Vozenilek et al., 2018). LDL receptor knockout ($Ldlr^{-/-}$) mice (on a C57BL/6J [$Nnt^{-/-}$] background) are prone to atherosclerosis (Salerno et al., 2019). Comparative analysis of peritoneal macrophages from C57BL/6JUnib ($Nnt^{+/+}$) mice, C57BL/6J ($Nnt^{-/-}$) mice, and $Ldlr^{-/-}/Nnt^{-/-}$ mice suggested that ROS levels increased in the following order: $Nnt^{+/+}$ < $Nnt^{-/-}$ < $Ldlr^{-/-}/Nnt^{-/-}$ (Salerno et al., 2019). Moreover, $Nnt^{-/-}$ and $Ldlr^{-/-}/Nnt^{-/-}$ macrophages exhibited the following: (1) upregulation of mitochondrial biogenesis markers (peroxisome proliferator-activated receptor gamma coactivator 1-alpha, mitochondrial transcription factor A, and ETC complexes), (2) upregulation of inflammation markers [inducible nitric oxide synthase, interleukin-6 (IL-6) and (IL-1β)], and (3) a decreased GSH/GSSG ratio (Salerno et al., 2019). Upon modified LDL exposure, $Nnt^{-/-}$ and $Ldlr^{-/-}/Nnt^{-/-}$ macrophages displayed increased lipid accumulation and foam cell formation (a hallmark of atherosclerosis). This suggests that macrophage NNT activity is critical for delaying the atherogenesis (plaque formation) process (Salerno et al., 2019).

Analysis of NNT Function in Other Models

In addition to patient- and C57BL/6J mice-derived cells and/or tissues, various other models have been used to study the effect of altered NNT protein levels and function. Cancer-related cell models are discussed below (see section "Role of NNT in cancer cells").

Cell models

NNT knockdown (to 50% of normal) in a rat dopaminergic cell model (PC12) partially depolarized $\Delta\psi$, reduced the cellular ratios of NADPH/$NADP^+$, and stimulated cellular H_2O_2 release at relatively high external glucose concentrations (20–100 mM; Yin et al., 2012). This study further reported that NNT knockdown increased intracellular ROS levels (0 and 20 mM external glucose concentration), reduced mitochondrial OCR, and reduced cellular ATP content. Extracellular acidification rates and lactate levels were not affected by NNT knockdown, whereas the phosphorylation of c-Jun N-terminal kinase (JNK; activation) and PDH (deactivation) was increased (Yin et al., 2012). The latter was paralleled by reduced activity of succinyl-CoA (SucCoA)-transferase, a.k.a. succinyl-CoA:3-ketoacid coenzyme A transferase 1, lower cell viability, and increased apoptosis. A mechanism was proposed in which redox-sensitive JNK activation induces PDH inhibition, intrinsic apoptosis activation, and reduced cell viability. This not only links NNT malfunction to a more oxidized cellular redox state and decline in mitochondrial bioenergetics, but also connects it to other redox-sensitive cellular functions (Yin et al., 2012).

Knockdown of *Nnt* in immortalized rat dopaminergic (N27) cells induced a 94% reduction in *Nnt* mRNA levels, associated with a 74% drop in NNT activity (Lopert and Patel, 2014). NNT knockdown increased cellular $NADP^+$ and reduced cellular NADPH content, associated with a twofold increase in $NADP^+$/NADPH ratio. As a consequence, cellular GSH decreased and GSSG increased, paralleled by reduced H_2O_2 removal rates. NNT-deficient cells further displayed normal IDH activity, increased peroxiredoxin 3 (Prx3; a.k.a. mitochondrial thioredoxin-dependent peroxide reductase [PRDX3]), oxidation, and reduced OCR. These results suggest that NNT constitutes an importance between the Trx/Prx antioxidant system(s) and respiration/substrate-dependent H_2O_2 catabolism in N27 cells (Lopert and Patel, 2014).

Analysis of the homozygous *NNT* variant p.G866D (gene mutation not reported) revealed normal *NNT* mRNA expression in mononuclear peripheral blood cells (Bodoni et al., 2023). The CRISPR-Cas9 technique was applied to generate *NNT*-deficient H295R (adrenal) cells harboring the *NNT* variant p.G866D (Bodoni et al., 2023). These cells displayed normal viability, reduced NNT protein levels and mitochondrial mass, increased ROS levels, reduced cortisol/aldosterone secretion, and cholesterol lipid droplets (LDs) of decreased size/density. Expression of key steroidogenic enzyme/coenzyme genes was either increased (STAR, CYP11A1, CYP11B1) or decreased (CYPB11B2) in the *NNT*-deficient cells. In contrast to control cells, forskolin stimulation did not increase cortisol secretion in *NNT*-deficient cells.

Experiments with C3H/HeJ mice demonstrated that NNT is expressed and regulated in immune-related cells and macrophages suggesting a potential role of NNT in immune cell function (Ripoll et al., 2012). To study this hypothesis, mouse full-length *Nnt* cDNA was stably overexpressed in a macrophage-like cell line (RAW264.7). Although the extent of overexpression was not reported, NNT-overexpressing cells displayed reduced levels of ROS and NO during the inflammatory response. In the case of ROS, this effect was independent of NADPH oxidases. NNT-overexpressing cells displayed an increased GSH/GSSG ratio after stimulation with lipopolysaccharide (LPS), suggesting that GSSG to GSH conversion is increased. LPS-induced inflammatory cytokine production and activation of MAPK signaling pathways were reduced by NNT overexpression. Moreover, the latter impaired the intracellular killing of *E. coli*, compatible with NNT being important in macrophage bacterial clearance (Ripoll et al., 2012).

Treatment of colon epithelial cells (HT29) with a redox cycling quinone (menadione) increased NNT catalytic activity in a low-glucose (1.2 mM) medium. This is compatible with NNT-mediated NADH-to-NADPH conversion being important in NADPH generation under these conditions (Circu et al., 2011).

Angiotensin II treatment increased NNT protein levels and activity in human aortic endothelial cells, paralleled by a reduced OCR (Rao et al., 2020). NNT knockdown (to <10% of normal) did not affect $\Delta\psi$, whereas OCR and cellular ATP content were decreased, and ROS levels and GR and GPX activities were further increased. Lower NNT levels/activity were also associated with decreased cellular ratios of $NADPH/NADP^+$ and increased cellular ratios of $NAD^+/NADH$ (Rao et al., 2020). NNT knockdown stimulated phosphorylation of the endothelial nitric oxide synthase (eNOS). These data suggest that NNT is required for phosphorylation-dependent regulation of eNOS activity (Rao et al., 2020).

Treatment with palmitate (C16; saturated), but not oleate (C18; unsaturated), reduced cellular NNT protein levels in αCD3/αCD28-stimulated PBMCs (McCambridge et al., 2019). NNT knockdown (to <20% of normal) reduced NADPH levels and increased the amount of ROS and Th17 cytokine production. It was proposed that palmitate regulates NNT function to alter immune cell function *via* redox-linked pathways (McCambridge et al., 2019).

Caenorhabditis elegans

Deletion of *nnt-1* in *C. elegans* did not affect growth under normal laboratory conditions but induced a large drop in GSH/GSSG ratio (Arkblad et al., 2005). Inducing superoxide-related oxidative stress in this model severely impaired growth, suggesting a crucial role for *nnt-1* in oxidative stress defense.

Zebrafish

To better understand fetal alcohol spectrum disorders, the role of NNT in ethanol-induced teratogenesis (*i.e.,* the alteration of developmental processes and induction of congenital deformities) was investigated in a zebrafish (*Danio rerio*) model (Mazumdar and Eberhart, 2023). A CRISPR-Cas9 *nnt* mutant (harboring a 74 bp deletion and premature termination sequence) displayed higher ROS levels relative to WT animals. Upon ethanol treatment, *nnt* mutants displayed increased brain and neuronal crest apoptosis, which was rescued by the GSH-precursor N-acetyl cysteine (NAC). This antioxidant also prevented most alcohol-induced craniofacial malformations. These results suggest that Nnt-mediated oxidative stress prevention protects against apoptosis and alcohol-induced teratogenesis (Mazumdar and Eberhart, 2023).

Role of NNT in Cancer Cells

Although detailed experimental information on the potential role of NNT in cancer cell function is currently still limited, it was proposed that the NNT dimer docks to CI near to its NADPH-binding site and its FMN-a site (Albracht et al., 2011). In this way, NNT could regulate the local $NADPH/NADP^+$ ratio and NADPH supply to CI in a $\Delta\psi$-dependent manner, and O_2 reaching the FMN-a site is converted into H_2O_2, which escapes CI (Albracht et al., 2011). As a consequence, the interplay between specific CI-mediated H_2O_2 production and specific NNT-mediated H_2O_2 removal, could affect apoptosis, autophagy, and cancer cell survival (Albracht et al., 2011). However, evidence in the aerobic yeast *Yarrowia lipolytica*, where NADPH-binding is mediated by the 39-kDa/NUEM accessory subunit of CI, revealed that bound NADPH is not involved in CI catalytic function but in CI stabilization (Fig. 7; Abdrakhmanova et al., 2006).

NNT and reductive carboxylation

As part of the TCA cycle, isocitrate is normally converted into α-KG by IDH1/IDH2-catalyzed oxidative decarboxylation. This reaction is reversible, allowing the generation of isocitrate from α-KG by reductive carboxylation, which is of great relevance for tumor cells (Mullen et al., 2014; He et al., 2022). Reductive carboxylation is a biochemical pathway to meet the increased demand for glutamine-derived carbons to support cellular anabolism in rapidly proliferating (*e.g.,* cancer) cells (Gameiro et al., 2013). Within mitochondria, reductive carboxylation constitutes a "reversed" reaction in which glutamine enters the TCA cycle in the form of α-KG, which is then reductively carboxylated to isocitrate in an IDH2-dependent manner. This mechanism (Fig. 7): (1) supports citrate production from isocitrate (reverse TCA reaction), (2) α-KGDG-catalyzed formation of SucCoA and succinate from α-KG (forward TCA reaction), and (3) requires conversion of NADPH into $NADP^+$ and of NAD^+ into NADH. In this way, the reductive carboxylation pathway provides cancer cells with an important cellular carbon source for FA synthesis (from citrate) during conditions of hypoxia and/or mitochondrial dysfunction (Fendt et al., 2013; Gameiro et al., 2013; Alberghina and Gaglio, 2014; Mullen et al., 2014; Jiang et al., 2023). Reductive carboxylation is activated by an increased α-ketoglutarate/citrate ratio (Fendt et al., 2013). Compatible with its $NADP^+$- and NADH-consuming and NADPH and NAD^+-generating function (Fig. 7), NNT knockdown inhibited reductive carboxylation in SkMel5 (melanoma) and 786-O (renal carcinoma) cell models (Gameiro et al., 2013). This knockdown was paralleled by a lower cellular $NADPH/NADP^+$ ratio, a mild increase in PPP activity, reduced glutamine entry into the TCA cycle, glycolysis activation, and increased isocitrate and citrate levels. However, NNT knockdown did not affect the isocitrate/citrate to α-KG ratio. Conversely, NNT overexpression increased $NADPH/NADP^+$ ratio, stimulated reductive carboxylation and glutamine oxidation, and reduced glucose catabolism in the TCA cycle (Gameiro et al., 2013). Unexpectedly, NNT knockdown decreased the cellular $NADH/NAD^+$ ratio and increased the lactate/pyruvate ratio. This was attributed to the fact that the measured $NADH/NAD^+$ ratio primarily reflects the cytosolic and not the mitochondrial situation. Taken together, these findings support the conclusion that NNT fulfills a coordinating role in determining the balance between glucose and glutamine utilization in the investigated cancer cell models (Gameiro et al., 2013). Directly below we summarize NNT-focused studies for specific cancer types.

Adrenocortical carcinoma

Adrenocortical carcinoma (ACC) is an aggressive malignancy with poor response to chemotherapy (Chortis et al., 2018). In an effort to induce oxidative stress and ensuing cell death, NNT was transiently knocked down in ACC cells (NCI-H295R). This knockdown suppressed cell proliferation, stimulated apoptosis, sensitized the cells to exogenous oxidative stress, and unexpectedly, stimulated steroidogenesis (Chortis et al., 2018). In a chronic model, stable NNT knockdown and long-term culture yielded cells

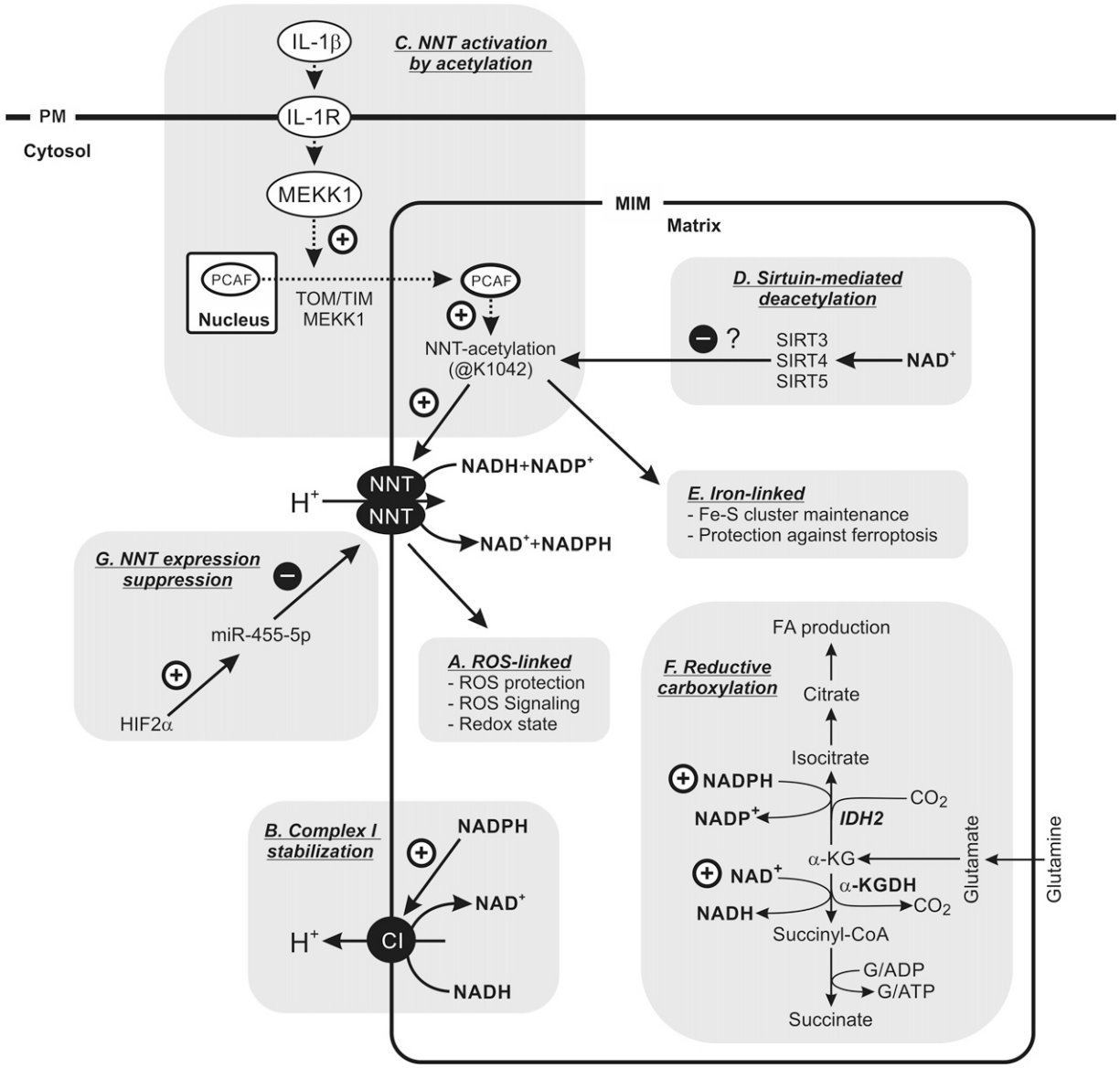

FIG. 7. Role of NNT in cancer cell energy metabolism and redox homeostasis. **(A)** Function of NNT in ROS-linked pathways. **(B)** Potential role of NADPH in CI stabilization. **(C)** PCAF-mediated NNT acylation (activation) pathway. **(D)** Potential sirtuin-mediated deactivation of NNT. **(E)** Role of NNT in Fe-linked pathways. **(F)** Role of NNT in reductive carboxylation by supplying NADPH and NAD^+. **(G)** Suppression of NNT expression by HIF2α. See main text for details. CI, complex I; HIF2α, hypoxia-inducible factor subunit; PCAF, p300/CBP-associated factor.

that were still proliferation-suppressed but displayed adaptive responses associated with a restored redox balance, restored oxidative stress resilience, and increased OCR. Transcriptome and metabolome analysis suggested that adaptation was paralleled by major changes in nucleotide synthesis, protein folding, and polyamine metabolism (Chortis et al., 2018). This preclinical evidence suggests that reducing NNT levels and/or increasing oxidative stress levels trigger a long-term adaptive response in ACC cells.

Clear cell renal cell carcinoma

Accumulation of LDs and activation of hypoxia-inducible factor (HIF) by loss of the von Hippel–Lindau factor are major characteristics in the progression of clear cell renal cell carcinoma (ccRCC; Xiong et al., 2021). HIF and ROS both decrease the expression of OXPHOS proteins in ccRCC cells, paralleled by alterations in mitochondrial redox homeostasis (Hervouet et al., 2008). During ccRCC oncogenesis, the HIF subunits HIF1α and HIF2α play a regulatory role, with HIF1α acting as a tumor suppressor and HIF2α acting as an oncogene promoting cell proliferation, metabolic alterations, and lipid accumulation (for refs see: Xiong et al., 2021). In human adipose tissue, white adipose tissue (WAT) is used to store energy, whereas brown adipose tissue (BAT) generates heat (Lee et al., 2014). Conversion of WAT into BAT (lipid browning) represents a mechanism in which stored lipids (WAT) are converted to energy (BAT). Interestingly, a similar reaction can occur in tumors upon conversion of LDs, which is not paralleled by increased ATP production

and associated with inhibited tumor progression. This process was named tumor cell "slimming" (Xiong et al., 2021). NNT mRNA/protein levels were reduced in ccRCC cell models and ccRCC patient tissues and predicted a poor prognosis in the latter. A mechanism was proposed (Fig. 7), in which HIF2α stimulates the expression of a microRNA (miR-455-5p). On its turn, miR-455-5p suppresses NNT expression and thereby inhibits NNT-mediated LD conversion and tumor slimming, leading to ccRCC progression (Xiong et al., 2021).

Gastric cancer

Increased *NNT* gene and protein expression in gastric cancer (GC) patient samples was paralleled by a shorter overall and disease-free survival (Li et al., 2018). Surprisingly, analysis of GC cell lines (HGC27, BGC823) demonstrated that NNT knockdown did not affect NADPH/$NADP^+$ and GSH/GSSG. However, when performing NNT knockdown in a glucose-free medium, NADPH/$NADP^+$ and GSH/GSSG ratios decreased, ROS levels increased, and apoptosis increased. The latter was characterized by increased cleavage of poly (ADP-ribose) polymerase and caspase 3 and was prevented by the antioxidant NAC (Li et al., 2018). In the same two cell lines, programmed cell death upon cell detachment (anoikis) induced an ROS increase. Under these conditions, NNT knockdown decreased NADPH/$NADP^+$ and GSH/GSSG ratios and increased ROS levels. In a xenograft model, NNT knockdown reduced *in vivo* tumor growth, suggesting that NNT inhibition might be a useful intervention in GC (Li et al., 2018).

In studying the promoting role of IL-1β in tumor progression, it was found that IL-1β stimulated the acylation of NNT at lysine K1042 (K1042ac) in MGC803 GC cells (Han et al., 2023). This lysine is located close to the C-terminus of the NNT protein (Fig. 2) within the matrix-localized NAD(P)H binding (dIII) domain (Fig. 3). NNT acetylation at K1042 was mediated by the histone acetyltransferase PCAF (p300/CBP-associated factor), which increased the $NADP^+$ binding affinity (*i.e.,* reduced the K_D value eightfold) and NNT activity (*i.e.,* NADPH production). PCAF massively translocated from the nucleus to mitochondria upon IL-1β stimulation, probably entering mitochondria *via* the translocase of the MOM complex by a mechanism involving mitogen-activated protein kinase kinase kinase 1(MEKK1; Han et al., 2023). Interestingly, analysis of the PCAF protein sequence revealed a putative MTS (first 85 amino acids), the deletion of which prevented IL-1β-stimulated nucleus-to-mitochondria PCAF translocation. Given the presence of this MTS, it remains to be determined why PCAF localization was primarily nuclear (and not mitochondrial) in the absence of IL-1β stimulation. Preventing K1042 acetylation by introducing a K1042R mutation greatly reduced IL-1β-induced NNT acetylation, suggesting that this PTM is the main NNT acetylation site. Surprisingly, increased K1042 acetylation did not alter mitochondrial ROS levels and Trx2/Grx2/Prx3/Prx5 redox status. This suggests that this acetylation does not induce redox and/or ROS stress (Han et al., 2023). Conversely, it was demonstrated that K1042 acetylation was linked to the maintenance of iron–sulfur (Fe-S) clusters and protection of the tumor cells from ferroptotic cell death (Fig. 7). These findings suggest that NNT acetylation is involved in the mechanism of IL-1β-promoted tumor immune evasion (Han et al., 2023).

Hepatocellular carcinoma

Data sets from The Cancer Genome Atlas (TCGA) cohort and Gene Expression Omnibus (GEO) revealed that NNT expression was reduced in patients with hepatocellular carcinoma (HCC), relative to control subjects (Duan et al., 2020). Survival analysis, quantitative polymerase chain reaction (qPCR), protein expression data, and *in silico* evidence demonstrated that low NNT expression was significantly associated with a poor prognosis and suggested that NNT activity was linked to bile acid functions and FA metabolism. It was proposed that downregulated NNT expression could serve as a prognostic biomarker for HCC (Duan et al., 2020).

A hepatoma cell model (SK-Hep-1) was used to study the roles of NADH and NADPH homeostasis in cancer (Ho et al., 2017). Virtually complete NNT knockdown reduced cell growth and tumorigenicity, reduced cellular NADPH levels, increased cellular NADH levels, increased OCR, increased ROS levels, increased cellular ATP content, reduced lactate production and $\Delta\psi$ hyperpolarization, and a normal mitochondrial mass. Mitochondria isolated from NNT knockdown cells displayed an increased CI-driven OCR. Treatment with the CI inhibitor rotenone reduced cell viability to a slightly greater extent in NNT knockdown cells than in controls. In contrast, NNT knockdown was protective against cell death induced by the glycolysis-inhibitor 3-bromopyruvate (Ho et al., 2017). Taken together, these results suggest that NNT knockdown shifts the energy metabolism toward a more mitochondrion-dependent phenotype. In this sense, NNT knockdown induced a phenotype in which cell growth was more dependent on pyruvate than on glucose in the medium. Metabolically, NNT knockdown decreased the steady-state fluxes of glycolysis and TCA cycle but increased reductive carboxylation (see section "NNT and reductive carboxylation"). NNT knockdown cells also displayed an increased [α-KG]/[succinate] ratio, leading to a decrease in HIF1α level and regulated genes (Ho et al., 2017). Moreover, the reduced NADPH levels reduced and increased histone deacetylase 1 activity and p53 acetylation, respectively.

Nonsmall-cell lung cancer

Tumor formation and aggressiveness were enhanced by NNT in non-small-cell lung cancer (NSCLC) mouse models (Ward et al., 2020). NNT function loss did not induce oxidative stress but was associated with mitochondrial dysfunction due to a reduced activity of Fe-S cluster-containing proteins. This suggests that NNT plays a significant role in lung tumor biology by regulating Fe-S cluster proteins (Ward et al., 2020). In this sense, NNT acetylation and activation were also implicated in the maintenance of Fe-S clusters and protection against ferroptotic cell death in GC (see section "Gastric cancer"). In the treatment of NSCLC, DNA methylation has been identified to play a role in the acquired resistance against the chemotherapeutic agent cisplatin (Xu et al., 2023). Using a cisplatin-resistant model (A549/DDP cells), it was found that NNT was silenced by DNA hypermethylation.

Moreover, DNA hypermethylation positively correlated with poor prognosis in NSCLC patients (Xu et al., 2023). Conversely, NNT overexpression in A549/DDP cells increased cisplatin sensitivity and suppressed tumor malignancy. Apparently, these phenomena were not NADPH- and/or ROS-mediated but due to NNT-mediated inhibition of protective autophagy. It was suggested that NNT potentially reduced NAD^+ levels, leading to SIRT1 inactivation and inhibition of autophagy (Xu et al., 2023).

Summary, Conclusions, and Future Directions

NNT is a dimeric MIM protein that connects mitochondrial energy metabolism and redox homeostasis (Fig. 1). Currently, the mechanistic aspects of this connection, as well as the regulation of NNT activity, are still incompletely understood. Given the fact that the absence or knockdown of NNT variably impacts on the mitochondrial OCR, it appears that NNT is not always active. This suggests the existence of a control mechanism, which prevents too high NNT-mediated matrix proton influx and the ensuing impairment of mitochondrial OXPHOS. We expect that integrated live-cell quantification of NNT substrate levels and mitochondrial/cellular functional readouts will provide valuable new insights into the conditions under which NNT is active and how this activity relates to other metabolic and signaling pathways. Such a strategy would also allow a better dissection of local and/or compartment-specific (*i.e.,* mitochondrial matrix, cytosol, nucleus) effects of NNT (dys)function and enhance our understanding of how NNT dimerization is regulated. Both in humans and mice, NNT expression levels differ between tissues, suggesting that the downstream effects of *NNT/Nnt* mutations are tissue-specific. In this sense, the pathological mechanism in adrenal glands is rather

A. GCCD4 patients with *NNT* gene mutations

- Decreased/normal NNT protein levels
- Decreased NNT activity
- Decreased/normal mitochondrial mass
- Decreased mtDNA copy number
- Decreased CIV activity
- Decreased ATP content
- Decreased GSH levels
- Decreased viability upon exogenous H_2O_2
- Increased ROS levels
- Increased protein nitration
- No correlation between NNT mRNA and protein levels
- Fragmented mitochondrial structure
- Normal mitochondrial OCR

B. C57BL/6J mice with *Nnt* gene deletion

- No NNT protein
- No NNT activity
- Decreased mtDNA copy number
- Decreased/normal mitochondrial mass
- Decreased CI, CIV, CV activity
- Decreased/normal mitochondrial OCR
- Decreased mitochondrial $NADP^+$ reduction
- Decreased GSH/GSSG ratio
- Decreased aconitase activity
- Decreased mitochondrial H_2O_2 removal
- Increased CAT levels (liver)
- Increased mitochondrial H_2O_2 release (CII-specific)
- Increased PDH phosporylation (inactivation)
- Increased oxidative stress
- Increased susceptibility for mPTP opening
- Increased mitochondrial biogenesis
- Increased sensitivity to exogenous oxidative stress
- NNT reverse-mode action during CF
- Normal basal mitochondrial H^+ leak

C. Cell models

NNT knockdown or CRISPR/Cas9 (*NNT* mutation)

- Decreased NNT protein levels
- Decreased mitochondrial OCR
- Decreased cellular ATP content
- Decreased mitochondrial mass
- Decreased cellular NADPH/$NADP^+$ ratio
- Decreased cellular GSH/GSSG ratio
- Decreased LD size/density
- Decreased CYPB11B2 expression
- Decreased cellular H_2O_2 removal
- Decreased FSK-induced cortisol secretion
- Increased STAR, CYP11A1, CYP11B1 expression
- Increased PDH phosporylation (inactivation)
- Increased cellular ROS levels
- Increased cellular H_2O_2 release
- Increased apoptosis
- Partial $\Delta\psi$ depolarization
- Normal/decreased cell viability
- Normal ECAR and LAC levels
- **Cancer cells:** decreased reductive carboxylation
- **Cancer cells:** decreased GLN entry in TCA cycle
- **Cancer cells:** decreased cellular NADPH/$NADP^+$ ratio
- **Cancer cells:** decreased GSH/GSSH ratio
- **Cancer cells:** decreased cell proliferation
- **Cancer cells:** decreased tumorigencity
- **Cancer cells:** decreased LAC production
- **Cancer cells:** increased PPP activity
- **Cancer cells:** increased glycolysis
- **Cancer cells:** increased isocitrate and CYT levels
- **Cancer cells:** increased apoptosis / PARP cleavage
- **Cancer cells:** increased sensitivity to oxidative stress
- **Cancer cells:** increased ROS levels
- **Cancer cells:** increased mitochondrial OCR
- **Cancer cells:** increased cellular ATP content
- **Cancer cells:** $\Delta\psi$ hyperpolarization
- **Cancer cells:** normal mitochondrial mass

NNT (stable) overexpression

- Increased NNT protein levels
- Decreased ROS levels
- Decreased NO levels
- Increased GSH to GSSG conversion
- **Cancer cells:** decreased glucose catabolism in TCA cycle
- **Cancer cells:** increased reductive carboxylation
- **Cancer cells:** increased GLN oxidation

FIG. 8. Key cellular consequences of NNT dysfunction. **(A)** Alterations in cells from GCCD4 patients with *NNT* mutations. **(B)** Alterations in tissues/cells/mitochondria from C57BL/6J mice with an *Nnt* gene mutation. **(C)** Effects of NNT knockdown/overexpression in cell models. Results obtained in cancer cell models are highlighted in bold. See main text for details. GCCD4, glucocorticoid deficiency 4.

well understood (Fig. 6). Several studies demonstrated that C57BL/6J mice lack NNT protein, but the picture is less clear for patients with *NNT* mutations (Fig. 8A, B). This means that it still needs to be clarified whether the reported *NNT* mutations exert their pathogenic effects *via* NNT catalytic impairment and/or *via* lowering NNT protein levels. The absence of NNT in various C57BL/6J strains does not result in an obvious phenotype, but it seems to enhance sensitivity to metabolic stress (*e.g.,* an HFD). However, in-depth analyses of the adrenal cortex and glucocorticoid/mineralocorticoid levels in C57BL/6J mice are currently lacking. In this context, the development of mice with a conditional NNT deletion, cell-reprogramming based adrenal models, and/or NNT-specific chemical inhibitors/activators would be useful from a translational perspective. The role of NNT in tumorigenesis and cancer cell biology is still unclear and it may be useful to screen isogenic mouse strains with and without NNT for tumor incidence. Nevertheless, both in patients and in mice *NNT*/*Nnt* mutations induced various common aberrations at the cellular level (Fig. 8A, B), several of which were mimicked by NNT knockdown/overexpression in cancer cells (Fig. 8C). For example, evidence was provided that NNT function was linked to cancer cell ROS/redox homeostasis (protection and signaling), CI stabilization, Fe-linked pathways (Fe-S cluster maintenance, ferroptosis), and reductive carboxylation (Fig. 7). At the regulatory level, *NNT* gene expression in cancer cells was suppressed by HIF2a/miR-455-5p and NNT was activated *via* an IL-1β-/MEKK1/PCAF-dependent acetylation mechanism. Obviously, these results strongly depend on the experimental conditions, both in mice (*e.g.,* diet, housing conditions) and in cell models (*e.g.,* cell type, degree of knockdown/overexpression, type, and concentration of energy substrates in the medium). Moreover, data from intact cells and isolated mitochondria cannot always directly be compared (*e.g.,* due to the presence/absence of cytosolic enzymes/substrates). We conclude that the emerging central role of NNT in linking adaptive regulation of redox homeostasis to energy metabolism warrants further research to improve our mechanistic understanding of its functional role and regulation.

Acknowledgments

The authors apologize to those authors whose articles they were unable to cite because of space limitations.

Authors' Contributions

All authors contributed to the writing of the manuscript. J.K. and W.J.H.K. supervised the writing and finalized the manuscript text.

Author Disclosure Statement

The authors declare no competing financial interest.

Funding Information

Z.G. and W.J.H.K. are supported by the Next Level Animal Sciences (NLAS) initiative ("Data and Models") of Wageningen University (Wageningen, The Netherlands). W.L., L.H., and J.S. are supported by the China Scholarship Council (CSC; #201908110278). W.J.H.K. is supported by RGL (Research Group Leader) funding (Radboudumc, Nijmegen, The Netherlands). D.Z. is supported by a Netherlands research council VENI talent grant (09150161910179).

References

Abdrakhmanova A, Zwicker K, Kerscher S, et al. Tight binding of NADPH to the 39-kDa subunit of complex I is not required for catalytic activity but stabilizes the multiprotein complex. Biochim Biophys Acta 2006;1757(12):1676–1682; doi: 10.1016/j.bbabio.2006.09.003

Alberghina L, Gaglio D. Redox control of glutamine utilization in cancer. Cell Death Dis 2014;5(12):e1561.

Albracht SP, Meijer AJ, Rydström J. Mammalian NADH: Ubiquinone oxidoreductase (Complex I) and nicotinamide nucleotide transhydrogenase (Nnt) together regulate the mitochondrial production of H_2O_2–implications for their role in disease, especially cancer. J Bioenerg Biomembr 2011;43(5):541–564; doi: 10.1007/s10863-011-9381-4

Allouche J, Rachmin I, Adhikari K, et al. NNT mediates redox-dependent pigmentation via a UVB- and MITF-independent mechanism. Cell 2021;184(16):4268–4283.e20; doi: 10.1016/j.cell.2021.06.022PMC8349839

Arkblad EL, Tuck S, Pestov NB, et al. A Caenorhabditis elegans mutant lacking functional nicotinamide nucleotide transhydrogenase displays increased sensitivity to oxidative stress. Free Radic Biol Med 2005;38(11):1518–1525; doi: 10.1016/j.freeradbiomed.2005.02.012

Ashkenazy H, Abadi S, Martz E, et al. ConSurf 2016: An improved methodology to estimate and visualize evolutionary conservation in macromolecules. Nucleic Acids Res 2016; 44(W1):W344–W50; doi: 10.1093/nar/gkw408

Bainbridge MN, Davis EE, Choi WY, et al. Loss of function mutations in NNT are associated with left ventricular non-compaction. Circ Cardiovasc Genet 2015;8(4):544–552; doi: 10.1161/CIRCGENETICS.115.001026

Beli P, Lukashchuk N, Wagner SA, et al. Proteomic investigations reveal a role for RNA processing factor THRAP3 in the DNA damage response. Mol Cell 2012;46(2):212–225; doi: 10.1016/j.molcel.2012.01.026

Bicego R, Francisco A, Ruas JS, et al. Undesirable effects of chemical inhibitors of NAD(P)+ transhydrogenase on mitochondrial respiratory function. Arch Biochem Biophys 2020; 692:108535; doi: 10.1016/j.abb.2020.108535

Blacker TS, Mann ZF, Gale JE, et al. Separating NADH and NADPH fluorescence in live cells and tissues using FLIM. Nat Commun 2014;5:3936; doi: 10.1038/ncomms4936

Bodoni AF, Coeli-Lacchini FB, Gebenlian JL, et al. Nicotinamide nucleotide transhydrogenase is essential for adrenal steroidogenesis: Clinical and *in vitro* lessons. J Clin Endocrinol Metab 2023;108(6):1464–1474; doi: 10.1210/clinem/dgac705

Borkum JM. Brain energy deficit as a source of oxidative stress in migraine: A molecular basis for migraine susceptibility. Neurochem Res 2021;46(8):1913–1932; doi: 10.1007/s11064-021-03335-9

Boylston JA, Sun J, Chen Y, et al. Characterization of the cardiac succinylome and its role in ischemia-reperfusion injury. J Mol Cell Cardiol 2015;88:73–81; doi: 10.1016/j.yjmcc.2015.09.005

Bradshaw PC. Cytoplasmic and mitochondrial NADPH-coupled redox systems in the regulation of aging. Nutrients 2019; 11(3):504; doi: 10.3390/nu11030504

Bulthuis EP, Adjobo-Hermans MJW, Willems PHGM, et al. Mitochondrial morphofunction in mammalian cells. Antioxid Redox Signal 2019;30(18):2066–2109; doi: 10.1089/ars.2018.7534

Bulthuis EP, Einer C, Distelmaier F, et al. The decylTPP mitochondria-targeting moiety lowers electron transport chain supercomplex levels in primary human skin fibroblasts. Free Radic Biol Med 2022;188:434–446; doi: 10.1016/j.freeradbiomed.2022.06.011

Bulthuis EP, Dieteren CEJ, Bergmans J, et al. Stress-dependent macromolecular crowding in the mitochondrial matrix. Embo J 2023;42(7):e108533; doi: 10.15252/embj.2021108533

Busanello ENB, Figueira TR, Marques AC, et al. Facilitation of Ca^{2+}-induced opening of the mitochondrial permeability transition pore either by nicotinamide nucleotide transhydrogenase deficiency or statins treatment. Cell Biol Int 2018;42(6):742–746; doi: 10.1002/cbin.10949

Carrico C, Meyer JG, He W, et al. The mitochondrial acylome emerges: Proteomics, regulation by sirtuins, and metabolic and disease implications. Cell Metab 2018;27(3):497–512; doi: 10.1016/j.cmet.2018.01.016

Chen S, Guillory RJ. The reaction mechanism of the mitochondrial pyridine nucleotide transhydrogenase. A study utilizing arylazido-pyridine nucleotide analogues. J Biol Chem 1984;259(9):5945–5953.

Chen WW, Freinkman E, Wang T, et al. Absolute quantification of matrix metabolites reveals the dynamics of mitochondrial metabolism. Cell 2016;166(5):1324–1337.e11; doi: 10.1016/j.cell.2016.07.040

Chenna S, Koopman WJH, Prehn JHM, et al. Mechanisms and mathematical modeling of ROS production by the mitochondrial electron transport chain. Am J Physiol Cell Physiol 2022;323(1):C69–C83; doi: 10.1152/ajpcell.00455.2021

Chini CCS, Zeidler JD, Kashyap S, et al. Evolving concepts in NAD+ metabolism. Cell Metab 2021;33(6):1076–1087; doi: 10.1016/j.cmet.2021.04.003

Chortis V, Taylor AE, Doig CL, et al. Nicotinamide nucleotide transhydrogenase as a novel treatment target in adrenocortical carcinoma. Endocrinology 2018;159(8):2836–2849; doi: 10.1210/en.2018-00014

Choudhary C, Kumar C, Gnad F, et al. Lysine acetylation targets protein complexes and co-regulates major cellular functions. Science 2009;325(5942):834–840; doi: 10.1126/science.1175371

Ciapaite J, Bakker SJ, Diamant M, et al. Metabolic control of mitochondrial properties by adenine nucleotide translocator determines palmitoyl-CoA effects. Implications for a mechanism linking obesity and type 2 diabetes. Febs J 2006;273(23):5288–5302; doi: 10.1111/j.1742-4658.2006.05523.x

Circu ML, Maloney RE, Aw TY. Disruption of pyridine nucleotide redox status during oxidative challenge at normal and low-glucose states: Implications for cellular adenosine triphosphate, mitochondrial respiratory activity, and reducing capacity in colon epithelial cells. Antioxid Redox Signal 2011;14(11):2151–2162; doi: 10.1089/ars.2010.3489

Close AF, Chae H, Jonas JC. The lack of functional nicotinamide nucleotide transhydrogenase only moderately contributes to the impairment of glucose tolerance and glucose-stimulated insulin secretion in C57BL/6J vs C57BL/6N mice. Diabetologia 2021;64(11):2550–2561; doi: 10.1007/s00125-021-05548-7

Colak G, Pougovkina O, Dai L, et al. Proteomic and biochemical studies of lysine malonylation suggest its malonic aciduria-associated regulatory role in mitochondrial function and fatty acid oxidation. Mol Cell Proteomics 2015;14(11):3056–3071; doi: 10.1074/mcp.M115.048850

Console L, Scalise M, Giangregorio N, et al. The link between the mitochondrial fatty acid oxidation derangement and kidney injury. Front Physiol 2020;11:794; doi: 10.3389/fphys.2020.00794

Cotton NP, White SA, Peake SJ, et al. The crystal structure of an asymmetric complex of the two nucleotide binding components of proton-translocating transhydrogenase. Structure 2001;9(2):165–176; doi: 10.1016/s0969-2126(01)00571-8

Danielson L, Ernster L. Demonstration of a mitochondrial energy-dependent pyridine nucleotide transhydrogenase reaction. Biochem Biophys Res Commun 1963;10:91–96; doi: 10.1016/0006-291x(63)90274-2

de Magalhães JP. Distinguishing between driver and passenger mechanisms of aging. Nat Genet 2024;56(2):204–211; doi: 10.1038/s41588-023-01627-0

Dogar I, Dixon S, Gill R, et al. C57BL/6J mice upregulate catalase to maintain the hydrogen peroxide buffering capacity of liver mitochondria. Free Radic Biol Med 2020;146:59–69; doi: 10.1016/j.freeradbiomed.2019.10.409

Duan Z, Song Y, Zou X, et al. Nicotinamide nucleotide transhydrogenase acts as a new prognosis biomarker in hepatocellular carcinoma. Int J Clin Exp Pathol 2020;13(5):972–978.

Eriksson O, Fontaine E, Bernardi P. Chemical modification of arginines by 2,3-butanedione and phenylglyoxal causes closure of the mitochondrial permeability transition pore. J Biol Chem 1998;273(20):12669–12674; doi: 10.1074/jbc.273.20.12669

Favia M, Atlante A. Cellular redox state acts as switch to determine the direction of NNT-catalyzed reaction in cystic fibrosis cells. Int J Mol Sci 2021;22(2):967; doi: 10.3390/ijms22020967

Fendt SM, Bell EL, Keibler MA, et al. Reductive glutamine metabolism is a function of the α-ketoglutarate to citrate ratio in cells. Nat Commun 2013;4:2236; doi: 10.1038/ncomms3236

Fergusson G, Ethier M, Guévremont M, et al. Defective insulin secretory response to intravenous glucose in C57Bl/6J compared to C57Bl/6N mice. Mol Metab 2014;3(9):848–854; doi: 10.1016/j.molmet.2014.09.006

Figueira TR. A word of caution concerning the use of Nnt-mutated C57BL/6 mice substrains as experimental models to study metabolism and mitochondrial pathophysiology. Exp Physiol 2013;98(11):1643; doi: 10.1113/expphysiol.2013.074682

Figueira TR, Francisco A, Ronchi JA, et al. NADPH supply and the contribution of NAD(P)+ transhydrogenase (NNT) to H_2O_2 balance in skeletal muscle mitochondria. Arch Biochem Biophys 2021;707:108934; doi: 10.1016/j.abb.2021.108934

Figueira TR, Francisco A, Treberg JR, et al. Can NAD(P)+ transhydrogenase (NNT) mediate a physiologically meaningful increase in energy expenditure by mitochondria during H2O2 removal? J Biol Chem 2021;296:100377; doi: 10.1016/j.jbc.2021.100377

Fisher-Wellman KH, Lin CT, Ryan TE, et al. Pyruvate dehydrogenase complex and nicotinamide nucleotide transhydrogenase constitute an energy-consuming redox circuit. Biochem J 2015;467(2):271–280; doi: 10.1042/BJ20141447

Fisher-Wellman KH, Ryan TE, Smith CD, et al. A direct comparison of metabolic responses to high-fat diet in C57BL/6J and C57BL/6NJ Mice. Diabetes 2016;65(11):3249–3261; doi: 10.2337/db16-0291

Flores-Romero H, Dadsena S, García-Sáez AJ. Mitochondrial pores at the crossroad between cell death and inflammatory signaling. Mol Cell 2023;83(6):843–856; doi: 10.1016/j.molcel.2023.02.021

Forsmark-Andrée P, Persson B, Radi R, et al. Oxidative modification of nicotinamide nucleotide transhydrogenase in submitochondrial particles: Effect of endogenous ubiquinol. Arch Biochem Biophys 1996;336(1):113–120; doi: 10.1006/abbi.1996.0538

Francisco A, Ronchi JA, Navarro CDC, et al. Nicotinamide nucleotide transhydrogenase is required for brain mitochondrial redox balance under hampered energy substrate metabolism and high-fat diet. J Neurochem 2018;147(5):663–677; doi: 10.1111/jnc.14602

Francisco A, Engel DF, Figueira TR, et al. Mitochondrial NAD(P)(+) Transhydrogenase is unevenly distributed in different brain regions, and its loss causes depressive-like behavior and motor dysfunction in mice. Neuroscience 2020;440:210–229; doi: 10.1016/j.neuroscience.2020.05.042

Francisco A, Figueira TR, Castilho RF. Mitochondrial NAD(P)(+) Transhydrogenase: From molecular features to physiology and disease. Antioxid Redox Signal 2022;36(13–15):864–884; doi: 10.1089/ars.2021.0111

Francisco A, Goler AMY, Navarro CDC, et al. Lack of NAD(P)+ transhydrogenase activity in patients with primary adrenal insufficiency due to NNT variants. Eur J Endocrinol 2024;190(2):lvae011–l138; doi: 10.1093/ejendo/lvae011

Frayn KN, Evans R. 2019. Human Metabolism: a Regulatory Perspective, 4th ed. Wiley-Blackwell: USA.

Freeman HC, Hugill A, Dear NT, et al. Deletion of nicotinamide nucleotide transhydrogenase: A new quantitive trait locus accounting for glucose intolerance in C57BL/6J mice. Diabetes 2006;55(7):2153–2156; doi: 10.2337/db06-0358

Fritz KS, Galligan JJ, Hirschey MD, et al. Mitochondrial acetylome analysis in a mouse model of alcohol-induced liver injury utilizing SIRT3 knockout mice. J Proteome Res 2012;11(3):1633–1643; doi: 10.1021/pr2008384

Fujisawa Y, Napoli E, Wong S, et al. Impact of a novel homozygous mutation in nicotinamide nucleotide transhydrogenase on mitochondrial DNA integrity in a case of familial glucocorticoid deficiency. BBA Clin 2015;3:70–78; doi: 10.1016/j.bbacli.2014.12.003

Gameiro PA, Laviolette LA, Kelleher JK, et al. Cofactor balance by Nicotinamide Nucleotide Transhydrogenase (NNT) coordinates reductive carboxylation and glucose catabolism in the Tricarboxylic Acid (TCA) cycle. J Biol Chem 2013;288(18):12967–12977; doi: 10.1074/jbc.M112.396796PMC3642339

Ghosh D, Levault KR, Brewer GJ. Relative importance of redox buffers GSH and NAD(P)H in age-related neurodegeneration and Alzheimer disease-like mouse neurons. Aging Cell 2014;13(4):631–640; doi: 10.1111/acel.12216

Goldstein JM, Wagers AJ. What's in a (Sub)strain? Stem Cell Reports 2018;11(2):303–305; doi: 10.1016/j.stemcr.2018.07.011

Goodpaster BH, Sparks LM. Metabolic flexibility in health and disease. Cell Metab 2017;25(5):1027–1036; doi: 10.1016/j.cmet.2017.04.015

Graf SS, Hong S, Müller P, et al. Energy transfer between the nicotinamide nucleotide transhydrogenase and ATP synthase of Escherichia coli. Sci Rep 2021;11(1):21234; doi: 10.1038/s41598-021-00651-6

Grayson C, Mailloux RJ. Coenzyme Q10 and nicotinamide nucleotide transhydrogenase: Sentinels for mitochondrial hydrogen peroxide signaling. Free Radic Biol Med 2023;208:260–271; doi: 10.1016/j.freeradbiomed.2023.08.015

Guarente L. Franklin H. Epstein Lecture: Sirtuins, aging, and medicine. N Engl J Med 2011;364(23):2235–2244; doi: 10.1056/NEJMra1100831

Halliwell B, Gutteridge JMC. Free Radicals in Biology and Medicine. Oxford University Press; 2015.

Han Y, Zhang YY, Pan YQ, et al. IL-1β-associated NNT acetylation orchestrates iron-sulfur cluster maintenance and cancer immunotherapy resistance. Mol Cell 2023;83(11):1887–1902.e8; doi: 10.1016/j.molcel.2023.05.011

He Q, Chen J, Xie Z, et al. Wild-type isocitrate dehydrogenase-dependent oxidative decarboxylation and reductive carboxylation in cancer and their clinical significance. Cancers (Basel) 2022;14(23):5779; doi: 10.3390/cancers14235779

Heiker JT, Kern M, Kosacka J, et al. Nicotinamide nucleotide transhydrogenase mRNA expression is related to human obesity. Obesity (Silver Spring) 2013;21(3):529–534; doi: 10.1002/oby.20095

Hershkovitz E, Arafat M, Loewenthal N, et al. Combined adrenal failure and testicular adrenal rest tumor in a patient with nicotinamide nucleotide transhydrogenase deficiency. J Pediatr Endocrinol Metab 2015;28(9–10):1187–1190; doi: 10.1515/jpem-2015-0075

Hervouet E, Cízková A, Demont J, et al. HIF and reactive oxygen species regulate oxidative phosphorylation in cancer. Carcinogenesis 2008;29(8):1528–1537; doi: 10.1093/carcin/bgn125

Hirose M, Schilf P, Gupta Y, et al. Lifespan effects of mitochondrial mutations. Nature 2016;540(7633):E13–E14; doi: 10.1038/nature20778

Ho HY, Lin YT, Lin G, et al. Nicotinamide Nucleotide Transhydrogenase (NNT) deficiency dysregulates mitochondrial retrograde signaling and impedes proliferation. Redox Biol 2017;12:916–928; doi: 10.1016/j.redox.2017.04.035

Holden HM, Rayment I, Thoden JB. Structure and function of enzymes of the Leloir pathway for galactose metabolism. J Biol Chem 2003;278(45):43885–43888; doi: 10.1074/jbc.R300025200

Hu MC, Hsu HJ, Guo IC, et al. Function of Cyp11a1 in animal models. Mol Cell Endocrinol 2004;215(1–2):95–100; doi: 10.1016/j.mce.2003.11.024

Huang TT, Naeemuddin M, Elchuri S, et al. Genetic modifiers of the phenotype of mice deficient in mitochondrial superoxide dismutase. Hum Mol Genet 2006;15(7):1187–1194; doi: 10.1093/hmg/ddl034

Jackson JB. A review of the binding-change mechanism for proton-translocating transhydrogenase. Biochim Biophys Acta 2012;1817(10):1839–1846; doi: 10.1016/j.bbabio.2012.04.006

Iannetti EF, Smeitink JAM, Willems P, et al. Rescue from galactose-induced death of Leigh Syndrome patient cells by pyruvate and NAD. $^{+}$Cell Death Dis 2018;9(11):1135; doi: 10.1038/s41419-018-1179-4

Janssen Daalen JM, Koopman WJH, Saris CGJ, et al. The hypoxia response pathway: A potential intervention target in

Parkinson's disease? Mov Disord 2023;39(2):273–293; doi: 10.1002/mds.29688

Jazayeri O, Liu X, van Diemen CC, et al. A novel homozygous insertion and review of published mutations in the NNT gene causing Familial Glucocorticoid Deficiency (FGD). Eur J Med Genet 2015;58(12):642–649; doi: 10.1016/j.ejmg.2015.11.001

Jiang H, He CJ, Li AM, et al. Mitochondrial uncoupling inhibits reductive carboxylation in cancer cells. Mol Cancer Res 2023;21(10):1010–1016; doi: 10.1158/1541-7786.MCR-23-0049

Kaludercic N, Di Lisa F. The energetic cost of NNT-dependent ROS removal. J Biol Chem 2020;295(48):16217–16218; doi: 10.1074/jbc.H120.016368

Kampjut D, Sazanov LA. Structure and mechanism of mitochondrial proton-translocating transhydrogenase. Nature 2019;573(7773):291–295; doi: 10.1038/s41586-019-1519-2

Katsyuba E, Romani M, Hofer D, et al. NAD+ homeostasis in health and disease. Nat Metab 2020;2(1):9–31; doi: 10.1038/s42255-019-0161-5

Kim A, Chen CH, Ursell P, et al. Genetic modifier of mitochondrial superoxide dismutase-deficient mice delays heart failure and prolongs survival. Mamm Genome 2010;21(11–12):534–542; doi: 10.1007/s00335-010-9299-x

Koopman WJH, Nijtmans LG, Dieteren CE, et al. Mammalian mitochondrial complex I: Biogenesis, regulation, and reactive oxygen species generation. Antioxid Redox Signal 2010;12(12):1431–1470; doi: 10.1089/ars.2009.2743

Koopman WJH, Willems PHGM, Smeitink JAM. Monogenic mitochondrial disorders. N Engl J Med 2012;366(12):1132–1141; doi: 10.1056/NEJMra1012478

Kraev A. Parallel universes of black six biology. Biol Direct 2014;9:18; doi: 10.1186/1745-6150-9-18PMC4108611

Krasovec T, Sikonja J, Zerjav Tansek M, et al. Long-term follow-up of three family members with a novel NNT pathogenic variant causing primary adrenal insufficiency. Genes (Basel) 2022;13(5):717; doi: 10.3390/genes13050717

Krengel U, Törnroth-Horsefield S. Biochemistry. Coping with oxidative stress. Science 2015;347(6218):125–126; doi: 10.1126/science.aaa3602

Kunath A, Heiker JT, Kern M, et al. Nicotinamide Nucleotide Transhydrogenase (Nnt) is related to obesity in Mice. Horm Metab Res 2020;52(12):877–881; doi: 10.1055/a-1199-2257

Lee YH, Mottillo EP, Granneman JG. Adipose tissue plasticity from WAT to BAT and in between. Biochim Biophys Acta 2014;1842(3):358–369; doi: 10.1016/j.bbadis.2013.05.011

Leung JH, Schurig-Briccio LA, Yamaguchi M, et al. Structural biology. Division of labor in transhydrogenase by alternating proton translocation and hydride transfer. Science 2015;347(6218):178–181; doi: 10.1126/science.1260451

Latorre-Pellicer A, Moreno-Loshuertos R, Lechuga-Vieco AV, et al. Mitochondrial and nuclear DNA matching shapes metabolism and healthy ageing. Nature 2016;535(7613):561–565; doi: 10.1038/nature18618

Li S, Zhuang Z, Wu T, et al. Nicotinamide nucleotide transhydrogenase-mediated redox homeostasis promotes tumor growth and metastasis in gastric cancer. Redox Biol 2018;18:246–255; doi: 10.1016/j.redox.2018.07.017

Li M, Tian W, Wang F, et al. Nicotinamide nucleotide transhydrogenase mutation analysis in Chinese patients with thyroid dysgenesis. Am J Med Genet A 2022;188(1):89–98; doi: 10.1002/ajmg.a.62493

Li X, Qian K, Zhang Y, et al. Ubiquitin-Specific Peptidase 47 (USP47) regulates cutaneous oxidative injury through Nicotinamide Nucleotide Transhydrogenase (NNT). Toxicol Appl Pharmacol 2023;480:116734; doi: 10.1016/j.taap.2023.116734

Lin S, Xing H, Zang T, et al. Sirtuins in mitochondrial stress: Indispensable helpers behind the scenes. Ageing Res Rev 2018;44:22–32; doi: 10.1016/j.arr.2018.03.006

Liemburg-Apers DC, Schirris TJ, Russel FG, et al. Mitoenergetic dysfunction triggers a rapid compensatory increase in steady-state glucose flux. Biophys J 2015;109(7):1372–1386; doi: 10.1016/j.bpj.2015.08.002

Liemburg-Apers DC, Wagenaars JA, Smeitink JA, et al. Acute stimulation of glucose influx upon mitoenergetic dysfunction requires LKB1, AMPK, Sirt2 and mTOR-RAPTOR. J Cell Sci 2016;129(23):4411–4423; doi: 10.1242/jcs.194480

Lopert P, Patel M. Nicotinamide Nucleotide Transhydrogenase (Nnt) links the substrate requirement in brain mitochondria for hydrogen peroxide removal to the thioredoxin/peroxiredoxin (Trx/Prx) system. J Biol Chem 2014;289(22):15611–15620; doi: 10.1074/jbc.M113.533653

Maharaj A, Maudhoo A, Chan LF, et al. Isolated glucocorticoid deficiency: Genetic causes and animal models. J Steroid Biochem Mol Biol 2019;189:73–80; doi: 10.1016/j.jsbmb.2019.02.012

Mantel CR, O'Leary HA, Chitteti BR, et al. Enhancing hematopoietic stem cell transplantation efficacy by mitigating oxygen shock. Cell 2015;161(7):1553–1565; doi: 10.1016/j.cell.2015.04.054

Mazumdar R, Eberhart JK. Loss of Nicotinamide nucleotide transhydrogenase sensitizes embryos to ethanol-induced neural crest and neural apoptosis via generation of reactive oxygen species. Front Neurosci 2023;17:1154621; doi: 10.3389/fnins.2023.1154621

McCambridge G, Agrawal M, Keady A, et al. Saturated fatty acid activates T Cell inflammation through a Nicotinamide Nucleotide Transhydrogenase (NNT)-dependent mechanism. Biomolecules 2019;9(2):79; doi: 10.3390/biom9020079

Meimaridou E, Kowalczyk J, Guasti L, et al. Mutations in NNT encoding nicotinamide nucleotide transhydrogenase cause familial glucocorticoid deficiency. Nat Genet 2012;44(7):740–742; doi: 10.1038/ng.2299

Meimaridou E, Hughes CR, Kowalczyk J, et al. Familial glucocorticoid deficiency: New genes and mechanisms. Mol Cell Endocrinol 2013;371(1–2):195–200; doi: 10.1016/j.mce.2012.12.010

Meimaridou E, Goldsworthy M, Chortis V, et al. NNT is a key regulator of adrenal redox homeostasis and steroidogenesis in male mice. J Endocrinol 2018;236(1):13–28; doi: 10.1530/JOE-16-0638

Mekada K, Yoshiki A. Substrains matter in phenotyping of C57BL/6 mice. Exp Anim 2009;70(2):145–160; doi: 10.1538/expanim.20-0158

Mertins P, Qiao JW, Patel J, et al. Integrated proteomic analysis of post-translational modifications by serial enrichment. Nat Methods 2013;10(7):634–637; doi: 10.1038/nmeth.2518

Metherell LA, Guerra-Assunção JA, Sternberg MJ, et al. Three-dimensional model of human Nicotinamide Nucleotide Transhydrogenase (NNT) and sequence-structure analysis of its disease-causing variations. Hum Mutat 2016;37(10):1074–1084; doi: 10.1002/humu.23046

Midzak A, Papadopoulos V. Adrenal mitochondria and steroidogenesis: From individual proteins to functional protein assemblies. Front Endocrinol (Lausanne) 2016;7:106; doi: 10.3389/fendo.2016.00106

Miller WP. Role of mitochondria in steroidogenesis. Miller WL. Role of mitochondria in steroidogenesis. Endocr Dev 2011; 20:1–19; doi: 10.1159/000321204

Mitchell P, Moyle J. Chemiosmotic hypothesis of oxidative phosphorylation. Nature 1967;213(5072):137–139; doi: 10.1038/213137a0

Monné M, Miniero DV, Iacobazzi V, et al. The mitochondrial oxoglutarate carrier: From identification to mechanism. J Bioenerg Biomembr 2013;45(1–2):1–13; doi: 10.1007/s10863-012-9475-7

Morales-Hernandez A, Martinat A, Chabot A, et al. Elevated oxidative stress impairs hematopoietic progenitor function in C57BL/6 Substrains. Stem Cell Reports 2018;11(2):334–347; doi: 10.1016/j.stemcr.2018.06.011

Mullen AR, Hu Z, Shi X, et al. Oxidation of alpha-ketoglutarate is required for reductive carboxylation in cancer cells with mitochondrial defects. Cell Rep 2014;7(5):1679–1690; doi: 10.1016/j.celrep.2014.04.037

Müller M, Bischof C, Kapries T, et al. Right heart failure in mice upon pressure overload is promoted by mitochondrial oxidative stress. JACC Basic Transl Sci 2022;7(7):658–677; doi: 10.1016/j.jacbts.2022.02.018

Murphy MP. Mitochondrial thiols in antioxidant protection and redox signaling: Distinct roles for glutathionylation and other thiol modifications. Antioxid Redox Signal 2012;16(6): 476–495; doi: 10.1089/ars.2011.4289

Murphy MP. Redox modulation by reversal of the mitochondrial nicotinamide nucleotide transhydrogenase. Cell Metab 2015;22(3):363–365; doi: 10.1016/j.cmet.2015.08.012

Navarro SJ, Trinh T, Lucas CA, et al. The C57BL/6J mouse strain background modifies the effect of a mutation in Bcl2l2. G3 (Bethesda) 2012;2(1):99–102; doi: 10.1534/g3.111.000778

Navarro CDC, Figueira TR, Francisco A, et al. Redox imbalance due to the loss of mitochondrial NAD(P)-transhydrogenase markedly aggravates high fat diet-induced fatty liver disease in mice. Free Radic Biol Med 2017;113:190–202; doi: 10.1016/j.freeradbiomed.2017.09.026

Navarro CDC, Francisco A, Figueira TR, et al. Dichloroacetate reactivates pyruvate-supported peroxide removal by liver mitochondria and prevents NAFLD aggravation in NAD(P)+ transhydrogenase-null mice consuming a high-fat diet. Eur J Pharmacol 2022;917:174750; doi: 10.1016/j.ejphar.2022.174750

Navarro CDC, Francisco A, Costa EFD, et al. Aging-dependent mitochondrial bioenergetic impairment in the skeletal muscle of NNT-deficient mice. Exp Gerontol 2024;193:112465; doi: 10.1016/j.exger.2024.112465

Nesci S, Trombetti F, Pagliarani A. Nicotinamide nucleotide transhydrogenase as a sensor of mitochondrial biology. Trends Cell Biol 2020;30(1):1–3; doi: 10.1016/j.tcb.2019.11.001

Nemoto S, Kubota T, Ohno H. Metabolic differences and differentially expressed genes between C57BL/6J and C57BL/6N mice substrains. PLoS One 2022;17(12):e0271651; doi: 10.1371/journal.pone.0271651

Nguyen TT, Wong R, Menazza S, et al. Cyclophilin D modulates mitochondrial acetylome. Circ Res 2013;113(12): 1308–1319; doi: 10.1161/CIRCRESAHA.113.301867

Nicholson A, Reifsnyder PC, Malcolm RD, et al. Diet-induced obesity in two C57BL/6 substrains with intact or mutant nicotinamide nucleotide transhydrogenase (Nnt) gene. Obesity (Silver Spring) 2010;18(10):1902–1905; doi: 10.1038/oby.2009.477

Nickel AG, von Hardenberg A, Hohl M, et al. Reversal of mitochondrial transhydrogenase causes oxidative stress in heart failure. Cell Metab 2015;22(3):472–484; doi: 10.1016/j.cmet.2015.07.008

Niu X, Stancliffe E, Gelman SJ, et al. Cytosolic and mitochondrial NADPH fluxes are independently regulated. Nat Chem Biol 2023;19(7):837–845; doi: 10.1038/s41589-023-01283-9

Novoselova TV, Rath SR, Carpenter K, et al. NNT pseudoexon activation as a novel mechanism for disease in two siblings with familial glucocorticoid deficiency. J Clin Endocrinol Metab 2015;100(2):E350–E4; doi: 10.1210/jc.2014-3641

Obiozo UM, Brondijk TH, White AJ, et al. Substitution of tyrosine 146 in the dI component of proton-translocating transhydrogenase leads to reversible dissociation of the active dimer into inactive monomers. J Biol Chem 2007;282(50): 36434–36443; doi: 10.1074/jbc.M705433200

Olgun A. Converting NADH to NAD+ by nicotinamide nucleotide transhydrogenase as a novel strategy against mitochondrial pathologies during aging. Biogerontology 2009;10(4): 531–534; doi: 10.1007/s10522-008-9190-2

Onuchic L, Padovano V, Schena G, et al. The C-terminal tail of polycystin-1 suppresses cystic disease in a mitochondrial enzyme-dependent fashion. Nat Commun 2023;14(1):1790; doi: 10.1038/s41467-023-37449-1

Ormö M, Persson B, Rydström J. Correlation between active form and dimeric structure of mitochondrial nicotinamide nucleotide transhydrogenase from beef heart. J Bioenerg Biomembr 1992;24(6):611–615; doi: 10.1007/BF00762353

Pagliarini DJ, Calvo SE, Chang B, et al. A mitochondrial protein compendium elucidates complex I disease biology. Cell 2008;134(1):112–123; doi: 10.1016/j.cell.2008.06.016

Park J, Chen Y, Tishkoff DX, et al. SIRT5-mediated lysine desuccinylation impacts diverse metabolic pathways. Mol Cell 2013;50(6):919–930; doi: 10.1016/j.molcel.2013.06.001

Parker N, Vidal-Puig AJ, Azzu V, et al. Dysregulation of glucose homeostasis in nicotinamide nucleotide transhydrogenase knockout mice is independent of uncoupling protein 2. Biochim Biophys Acta 2009;1787(12):1451–1457; doi: 10.1016/j.bbabio.2009.06.005

Persson B, Berden JA, Rydström J, et al. ATP-driven transhydrogenase provides an example of delocalized chemiosmotic coupling in reconstituted vesicles and in submitochondrial particles. Biochim Biophys Acta 1987;894(2):239–251; doi: 10.1016/0005-2728(87)90193-9

Picard M, McManus MJ, Gray JD, et al. Mitochondrial functions modulate neuroendocrine, metabolic, inflammatory, and transcriptional responses to acute psychological stress. Proc Natl Acad Sci U S A 2015;112(48):E6614–E23; doi: 10.1073/pnas.1515733112

Pons Fernández N, Moriano Gutiérrez A, Taberner Pazos B, et al. A novel mutation in the NNT gene causing familial glucocorticoid deficiency, with a literature review. Ann Endocrinol (Paris) 2024;85(1):70–81; doi: 10.1016/j.ando.2023.05.011

Qu C, Keijer J, Adjobo-Hermans MJW, et al. The ketogenic diet as a therapeutic intervention strategy in mitochondrial disease. Int J Biochem Cell Biol 2021;138:106050; doi: 10.1016/j.biocel.2021.106050

Rao KNS, Shen X, Pardue S, et al. Nicotinamide nucleotide transhydrogenase (NNT) regulates mitochondrial ROS and endothelial dysfunction in response to angiotensin II. Redox Biol 2020;36:101650; doi: 10.1016/j.redox.2020.101650

Rardin MJ, Newman JC, Held JM, et al. Label-free quantitative proteomics of the lysine acetylome in mitochondria identifies substrates of SIRT3 in metabolic pathways. Proc Natl Acad Sci U S A 2013;110(16):6601–6606; doi: 10.1073/pnas.1302961110

Rauh D, Fischer F, Gertz M, et al. An acetylome peptide microarray reveals specificities and deacetylation substrates for all human sirtuin isoforms. Nat Commun 2013;4:2327; doi: 10.1038/ncomms3327

Rawle DJ, Le TT, Dumenil T, et al. Widespread discrepancy in Nnt genotypes and genetic backgrounds complicates granzyme A and other knockout mouse studies. Elife 2022;11:e70207; doi: 10.7554/eLife.70207

Regan T, Conway R, Bharath LP. Regulation of immune cell function by nicotinamide nucleotide transhydrogenase. Am J Physiol Cell Physiol 2022;322(4):C666–C673; doi: 10.1152/ajpcell.00607.2020

Rimal S, Tantray I, Li Y, et al. Reverse electron transfer is activated during aging and contributes to aging and age-related disease. EMBO Rep 2023;24(4):e55548; doi: 10.15252/embr.202255548

Ripoll VM, Meadows NA, Bangert M, et al. Nicotinamide nucleotide transhydrogenase (NNT) acts as a novel modulator of macrophage inflammatory responses. FASEB J 2012;26(8):3550–3562; doi: 10.1096/fj.11-199935

Roat R, Rao V, Doliba NM, et al. Alterations of pancreatic islet structure, metabolism and gene expression in diet-induced obese C57BL/6J mice. PLoS One 2014;9(2):e86815; doi: 10.1371/journal.pone.0086815

Ronchi JA, Figueira TR, Ravagnani FG, et al. A spontaneous mutation in the nicotinamide nucleotide transhydrogenase gene of C57BL/6J mice results in mitochondrial redox abnormalities. Free Radic Biol Med 2013;63:446–456; doi: 10.1016/j.freeradbiomed.2013.05.049

Ronchi JA, Francisco A, Passos LA, et al. The contribution of nicotinamide nucleotide transhydrogenase to peroxide detoxification is dependent on the respiratory state and counterbalanced by other sources of NADPH in liver mitochondria. J Biol Chem 2016;291(38):20173–20187; doi: 10.1074/jbc.M116.730473

Roucher-Boulez F, Mallet-Motak D, Samara-Boustani D, et al. NNT mutations: A cause of primary adrenal insufficiency, oxidative stress and extra-adrenal defects. Eur J Endocrinol 2016;175(1):73–84; doi: 10.1530/EJE-16-0056

Rydström J. Site-specific inhibitors of mitochondrial nicotinamide-nucleotide transhydrogenase. Eur J Biochem 1972;31(3):496–504; doi: 10.1111/j.1432-1033.1972.tb02557.x

Rydström J, Hoek JB, Ericson BG, et al. Evidence for a lipid dependence of mitochondrial nicotinamide nucleotide transhydrogenase. Biochim Biophys Acta 1976;430(3):419–425; doi: 10.1016/0005-2728(76)90017-7

Rydstrom J. Mitochondrial NADPH, transhydrogenase and disease. Biochim Biophys Acta 2006;1757(5–6):721–726; doi: 10.1016/j.bbabio.2006.03.010

Sakata Y, Cheng K, Mayama M, et al. Reconstitution of human adrenocortical specification and steroidogenesis using induced pluripotent stem cells. Dev Cell 2022;57(22):2566–2583.e8; doi: 10.1016/j.devcel.2022.10.010

Salerno AG, Rentz T, Dorighello GG, et al. Lack of mitochondrial NADP(H)-transhydrogenase expression in macrophages exacerbates atherosclerosis in hypercholesterolemic mice. Biochem J 2019;476(24):3769–3789; doi: 10.1042/BCJ20190543

Salvi M, Battaglia V, Brunati AM, et al. Catalase takes part in rat liver mitochondria oxidative stress defense. J Biol Chem 2007;282(33):24407–24415; doi: 10.1074/jbc.M701589200

Santos LRB, Muller C, de Souza AH, et al. NNT reverse mode of operation mediates glucose control of mitochondrial NADPH and glutathione redox state in mouse pancreatic β-cells. Mol Metab 2017;6(6):535–547; doi: 10.1016/j.molmet.2017.04.004

Sarraf SA, Raman M, Guarani-Pereira V, et al. Landscape of the PARKIN-dependent ubiquitylome in response to mitochondrial depolarization. Nature 2013;496(7445):372–376; doi: 10.1038/nature12043

Scalise M, Pochini L, Galluccio M, et al. Glutamine transport. From energy supply to sensing and beyond. Biochim Biophys Acta 2016;1857(8):1147–1157; doi: 10.1016/j.bbabio.2016.03.006

Schiaffino S, Reggiani C, Kostrominova TY, et al. Mitochondrial specialization revealed by single muscle fiber proteomics: Focus on the Krebs cycle. Scand J Med Sci Sports 2015;25 Suppl 4:41–48; doi: 10.1111/sms.12606

Sharaf MS, Stevens D, Kamunde C. Mitochondrial transition ROS spike (mTRS) results from coordinated activities of complex I and nicotinamide nucleotide transhydrogenase. Biochim Biophys Acta Bioenerg 2017;1858(12):955–965; doi: 10.1016/j.bbabio.2017.08.012

Sheeran FL, Rydström J, Shakhparonov MI, et al. Diminished NADPH transhydrogenase activity and mitochondrial redox regulation in human failing myocardium. Biochim Biophys Acta 2010;1797(6–7):1138–1148; doi: 10.1016/j.bbabio.2010.04.002

Shen Z, Wang B, Luo J, et al. Global-scale profiling of differential expressed lysine acetylated proteins in colorectal cancer tumors and paired liver metastases. J Proteomics 2016;142:24–32; doi: 10.1016/j.jprot.2016.05.002

Shimizu R, Sakazaki F, Okuno T, et al. Difference in glucose intolerance between C57BL/6J and ICR strain mice with streptozotocin/nicotinamide-induced diabetes. Biomed Res 2012;33(1):63–66; doi: 10.2220/biomedres.33.63

Sieprath T, Corne TD, Willems PHGM, et al. Integrated high-content quantification of intracellular ROS levels and mitochondrial morphofunction. Adv Anat Embryol Cell Biol 2016;219:149–177; doi: 10.1007/978-3-319-28549-8_6

Sies H, Berndt C, Jones DP. Oxidative Stress. Annu Rev Biochem 2017;86:715–748; doi: 10.1146/annurev-biochem-061516-045037

Simon MM, Greenaway S, White JK, et al. A comparative phenotypic and genomic analysis of C57BL/6J and C57BL/6N mouse strains. Genome Biol 2013;14(7):R82; doi: 10.1186/gb-2013-14-7-r82

Smith CD, Schmidt CA, Lin CT, et al. Flux through mitochondrial redox circuits linked to nicotinamide nucleotide transhydrogenase generates counterbalance changes in energy expenditure. J Biol Chem 2020;295(48):16207–16216; doi: 10.1074/jbc.RA120.013899

Smith CD, Schmidt CA, Fisher-Wellman KH, et al. Reply to Figueira et al.: Can NAD(P)+ transhydrogenase (NNT) mediate a physiologically meaningful increase in energy expenditure by mitochondria during H2O2 removal? J Biol Chem 2021;296:100378; doi: 10.1016/j.jbc.2021.100378

Sol EM, Wagner SA, Weinert BT, et al. Proteomic investigations of lysine acetylation identify diverse substrates of mitochondrial deacetylase sirt3. PLoS One 2012;7(12):e50545; doi: 10.1371/journal.pone.0050545

Surwit RS, Kuhn CM, Cochrane C, et al. Diet-induced type II diabetes in C57BL/6J mice. Diabetes 1988;37(9):1163–1167; doi: 10.2337/diab.37.9.1163

Svinkina T, Gu H, Silva JC, et al. Deep, quantitative coverage of the lysine acetylome using novel anti-acetyl-lysine antibodies and an optimized proteomic workflow. Mol Cell Proteomics 2015;14(9):2429–2440; doi: 10.1074/mcp.O114.047555

Szabo I, Szewczyk A. Mitochondrial ion channels. Annu Rev Biophys 2023;52:229–254; doi: 10.1146/annurev-biophys-092622-094853

Tao R, Zhao Y, Chu H, et al. Genetically encoded fluorescent sensors reveal dynamic regulation of NADPH metabolism. Nat Methods 2017;14(7):720–728; doi: 10.1038/nmeth.4306

Teixeira J, Basit F, Willems PHGM, et al. Mitochondria-targeted phenolic antioxidants induce ROS-protective pathways in primary human skin fibroblasts. Free Radic Biol Med 2021;163:314–324; doi: 10.1016/j.freeradbiomed.2020.12.023

Timmermans S, Libert C. Overview of inactivating mutations in the protein-coding genome of the mouse reference strain C57BL/6J. JCI Insight 2018;3(13):e121758; doi: 10.1172/jci.insight.121758

Toye AA, Lippiat JD, Proks P, et al. A genetic and physiological study of impaired glucose homeostasis control in C57BL/6J mice. Diabetologia 2005;48(4):675–686; doi: 10.1007/s00125-005-1680-z

Tretter L, Adam-Vizi V. Generation of reactive oxygen species in the reaction catalyzed by alpha-ketoglutarate dehydrogenase. J Neurosci 2004;24(36):7771–7778; doi: 10.1523/JNEUROSCI.1842-04.2004

Usami M, Okada A, Taguchi K, et al. Genetic differences in C57BL/6 mouse substrains affect kidney crystal deposition. Urolithiasis 2018;46(6):515–522; doi: 10.1007/s00240-018-1040-3

van de Ven RAH, Santos D, Haigis MC. Mitochondrial sirtuins and molecular mechanisms of aging. Trends Mol Med 2017;23(4):320–331; doi: 10.1016/j.molmed.2017.02.005

Vercesi AE, Castilho RF, Kowaltowski AJ, et al. Mitochondrial calcium transport and the redox nature of the calcium-induced membrane permeability transition. Free Radic Biol Med 2018;129:1–24; doi: 10.1016/j.freeradbiomed.2018.08.034

Vozenilek AE, Vetkoetter M, Green JM, et al. Absence of nicotinamide nucleotide transhydrogenase in C57BL/6J mice exacerbates experimental atherosclerosis. J Vasc Res 2018;55(2):98–110; doi: 10.1159/000486337

Wagner SA, Beli P, Weinert BT, et al. Proteomic analyses reveal divergent ubiquitylation site patterns in murine tissues. Mol Cell Proteomics 2012;11(12):1578–1585; doi: 10.1074/mcp.M112.017905

Wagner M, Bertero E, Nickel A, et al. Selective NADH communication from α-ketoglutarate dehydrogenase to mitochondrial transhydrogenase prevents reactive oxygen species formation under reducing conditions in the heart. Basic Res Cardiol 2020;115(5):53; doi: 10.1007/s00395-020-0815-1

Ward NP, Kang YP, Falzone A, et al. Nicotinamide nucleotide transhydrogenase regulates mitochondrial metabolism in NSCLC through maintenance of Fe-S protein function. J Exp Med 2020;217(6):e20191689; doi: 10.1084/jem.20191689

White SA, Peake SJ, McSweeney S, et al. The high-resolution structure of the NADP(H)-binding component (dIII) of proton-translocating transhydrogenase from human heart mitochondria. Structure 2000;8(1):1–12; doi: 10.1016/s0969-2126(00)00075-7

Weinberg SE, Sena LA, Chandel NS. Mitochondria in the regulation of innate and adaptive immunity. Immunity 2015;42(3):406–417; doi: 10.1016/j.immuni.2015.02.002

Weinberg-Shukron A, Abu-Libdeh A, Zhadeh F, et al. Combined mineralocorticoid and glucocorticoid deficiency is caused by a novel founder nicotinamide nucleotide transhydrogenase mutation that alters mitochondrial morphology and increases oxidative stress. J Med Genet 2015;52(9):636–641; doi: 10.1136/jmedgenet-2015-103078

Weinert BT, Schölz C, Wagner SA, et al. Lysine succinylation is a frequently occurring modification in prokaryotes and eukaryotes and extensively overlaps with acetylation. Cell Rep 2013;4(4):842–851; doi: 10.1016/j.celrep.2013.07.024

Willems PHGM, Rossignol R, Dieteren CE, et al. Redox homeostasis and mitochondrial dynamics. Cell Metab 2015;22(2):207–218; doi: 10.1016/j.cmet.2015.06.006

Williams JL, Paudyal A, Awad S, et al. Mylk3 null C57BL/6N mice develop cardiomyopathy, whereas Nnt null C57BL/6J mice do not. Life Sci Alliance 2020;3(4):e201900593; doi: 10.26508/lsa.201900593

Williams JL, Hall CL, Meimaridou E, et al. Loss of Nnt increases expression of oxidative phosphorylation complexes in C57BL/6J Hearts. Int J Mol Sci 2021;22(11); doi: 10.3390/ijms22116101

Wolf S, Hainz N, Beckmann A, et al. Brain damage resulting from postnatal hypoxic-ischemic brain injury is reduced in C57BL/6J mice as compared to C57BL/6N mice. Brain Res 2016;1650:224–231; doi: 10.1016/j.brainres.2016.09.013

Wong N, Blair AR, Morahan G, et al. The deletion variant of Nicotinamide Nucleotide Transhydrogenase (Nnt) does not affect insulin secretion or glucose tolerance. Endocrinology 2010;151(1):96–102; doi: 10.1210/en.2009-0887

Wu Q, Cheng Z, Zhu J, et al. Suberoylanilide hydroxamic acid treatment reveals crosstalks among proteome, ubiquitylome and acetylome in non-small cell lung cancer A549 cell line. Sci Rep 2015;5:9520; doi: 10.1038/srep09520

Yang W, Nagasawa K, Münch C, et al. Mitochondrial sirtuin network reveals dynamic SIRT3-Dependent deacetylation in response to membrane depolarization. Cell 2016;167(4):985–1000.e21; doi: 10.1016/j.cell.2016.10.016

Xiao W, Loscalzo J. Metabolic responses to reductive stress. Antioxid Redox Signal 2020;32(18):1330–1347; doi: 10.1089/ars.2019.7803

Xiong Z, Xiong W, Xiao W, et al. NNT-induced tumor cell "slimming" reverses the pro-carcinogenesis effect of HIF2a in tumors. Clin Transl Med 2021;11(1):e264; doi: 10.1002/ctm2.264

Xu C, Jiang S, Ma X, et al. CRISPR-based DNA methylation editing of NNT rescues the cisplatin resistance of lung cancer

cells by reducing autophagy. Arch Toxicol 2023;97(2): 441–456; doi: 10.1007/s00204-022-03404-0

Yamaguchi R, Kato F, Hasegawa T, et al. A novel homozygous mutation of the nicotinamide nucleotide transhydrogenase gene in a Japanese patient with familial glucocorticoid deficiency. Endocr J 2013;60(7):855–859; doi: 10.1507/endocrj.ej13-0024

Yang R, Yang C, Ma L, et al. Identification of purine biosynthesis as an NADH-sensing pathway to mediate energy stress. Nat Commun 2022;13(1):7031; doi: 10.1038/s41467-022-34850-0

Yin F, Sancheti H, Cadenas E. Silencing of nicotinamide nucleotide transhydrogenase impairs cellular redox homeostasis and energy metabolism in PC12 cells. Biochim Biophys Acta 2012;1817(3):401–409; doi: 10.1016/j.bbabio.2011.12.004

Xiao W, Wang RS, Handy DE, et al. NAD(H) and NADP(H) redox couples and cellular energy metabolism. Antioxid Redox Signal 2018;28(3):251–272; doi: 10.1089/ars.2017.7216

Ying W. NAD^+/NADH and $NADP^+$/NADPH in cellular functions and cell death: Regulation and biological consequences. Antioxid Redox Signal 2008;10(2):179–206; doi: 10.1089/ars.2007.1672

Yoo HC, Park SJ, Nam M, et al. A variant of SLC1A5 is a mitochondrial glutamine transporter for metabolic reprogramming in cancer cells. Cell Metab 2020;31(2):267–283.e12; doi: 10.1016/j.cmet.2019.11.020

Xu H, Zhou J, Lin S, et al. PLMD: An updated data resource of protein lysine modifications. J Genet Genomics 2017;44(5): 243–250; doi: 10.1016/j.jgg.2017.03.007

Zhao S, Xu W, Jiang W, et al. Regulation of cellular metabolism by protein lysine acetylation. Science 2010;327(5968): 1000–1004; doi: 10.1126/science.1179689

Zhu X, Liu X, Cheng Z, et al. Quantitative analysis of global proteome and lysine acetylome reveal the differential impacts of VPA and SAHA on HL60 Cells. Sci Rep 2016;6:19926; doi: 10.1038/srep19926

Address correspondence to:
Dr. Werner J.H. Koopman
Human and Animal Physiology
Wageningen University
PO Box 338
7600AH Wageningen
The Netherlands

E-mail: Werner.Koopman@wur.nl

Date of first submission to ARS Central, July 17, 2024; date of final revised submission, July 22, 2024; date of acceptance, July 22, 2024.

Abbreviations Used

α-KG = α-ketoglutarate (2-oxoglutarate)
α-KGDH = α-ketoglutarate dehydrogenase
$\Delta\psi$ = mitochondrial trans-MIM membrane potential
ΔpH = mitochondrial trans-MIM pH gradient
AcCoA = acetyl coenzyme A
ACC = adrenocortical carcinoma
ACTH = adrenocorticotropic hormone
ACTHR = adrenocorticotropic hormone receptor
AD = Alzheimer's disease
ADP = adenosine diphosphate
ATP = adenosine triphosphate
BAT = brown adipose tissue
C, CYTC = cytochrome-*c*
CAT = catalase
ccRCC = clear cell renal cell carcinoma
CF = cystic fibrosis
CI-CV = complex I–V
CM = cardiomyopathy
CoQ10 = coenzyme Q10
CS = citrate synthase
CuZnSOD = copper–zinc superoxide dismutase (SOD1)
CYP = cytochrome P450
DCA = dichloroacetate
DHODH = dihydroorotate dehydrogenase
DIO = diet-induced obesity
EcTH = *E. coli* transhydrogenase
eNOS = endothelial nitric oxide synthase
ETC = electron transport chain
ETF = electron-transferring flavoprotein
FA = fatty acid
FDX = ferredoxin
FDXR = ferredoxin reductase
FeS = iron–sulfur
FGD = familial glucocorticoid deficiency
G6PD = glucose-6-phosphate dehydrogenase
GC = gastric cancer
GCCD = glucocorticoid deficiency
GDH = glutamate dehydrogenase
G3P = glycerol-3-phosphate
GPDH = glycerol-3-phosphate dehydrogenase
GPX = glutathione peroxidase
GR = glutathione reductase
GSH = glutathione
GSIS = glucose-stimulated insulin secretion
GSSG = oxidized glutathione
H_2O = water
H_2O_2 = hydrogen peroxide
HCC = hepatocellular carcinoma
HF = heart failure
HFD = high-fat diet
HIF = hypoxia-inducible factor
HSPC = hematopoietic stem and progenitor cell
IDH = isocitrate dehydrogenase
IL-1β = interleukin-1β
IL-1R = interleukin-1 receptor
IL-6 = interleukin-6
IMS = intermembrane space
LD = lipid droplet
LDL = low-density lipoprotein
LPS = lipopolysaccharide
MAL = malate
MCR2 = melanocortin 2 receptor
ME = malic enzyme
MEKK1 = mitogen-activated protein kinase kinase kinase 1(MAP3K1)
MIM = mitochondrial inner membrane
MOM = mitochondrial outer membrane
mPTP = mitochondrial permeability transition pore

Abbreviations Used (Cont.)

MRAP = melanocortin 2 receptor accessory protein
MTS = mitochondrial targeting sequence
MYLK = myosin light chain kinase 3
NAC = *N*-acetyl cysteine
NAD^+ = oxidized form of nicotinamide adenine dinucleotide
NADH = reduced form of nicotinamide adenine dinucleotide
$NADP^+$ = oxidized form of nicotinamide adenine dinucleotide phosphate
NADPH = reduced form of nicotinamide adenine dinucleotide phosphate
NAFLD = non-alcoholic fatty liver disease
NF = nonfailing
NNT = nicotinamide nucleotide transhydrogenase
NO = nitric oxide
NQO1 = NAD(P)H: quinone oxidoreductase 1
NSCLC = non-small-cell lung cancer
$O_2^{\bullet-}$ = superoxide
OCR = oxygen consumption rate
OXPHOS = oxidative phosphorylation
Palm-CoA = palmityl-coenzyme A (a.k.a. palmitoyl-coenzyme A)
PBMCs = peripheral blood mononuclear cells
PC1 = polycistin-1
PCAF = p300/CBP-associated factor
PDH = pyruvate dehydrogenase
PDHC = pyruvate dehydrogenase complex
P_i = inorganic phosphate
PIC = phosphate carrier
PID = percentage identity
PMF = proton-motive force
PPP = pentose phosphate pathway
PRDX3 = peroxiredoxin 3
PTMs = post-translational modifications
RET = reverse-electron transfer
ROS = reactive oxygen species
SIRT = sirtuin
SOD = superoxide dismutase
SucCoA = succinyl CoA
TCA = tricarboxylic acid
TRX = thioredoxin
TRXR2 = thioredoxin reductase 2
WAT = white adipose tissue